Chapter 4

Applications of the Josephson Effect

II. Applications of the Josephson Effect

Motivation for analog and digital applications

$I_s^m = I_s^m(B)$
→ Superconducting quantum interference device (Magnetic field sensors) (Ch. 4)

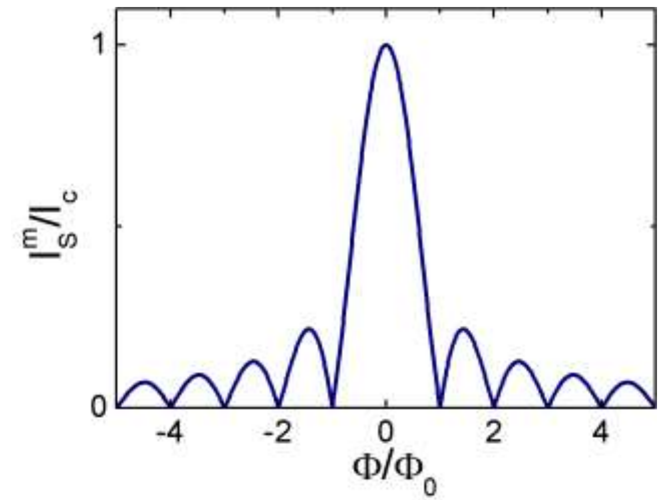

$\beta_C \gg 1$
→ Zero/finite voltage state bistability
→ Switching devices, Josephson computer (ch. 5)

2nd Josephson equation $\frac{d\varphi}{dt} = 2eV/\hbar$
→ VCO, voltage standard

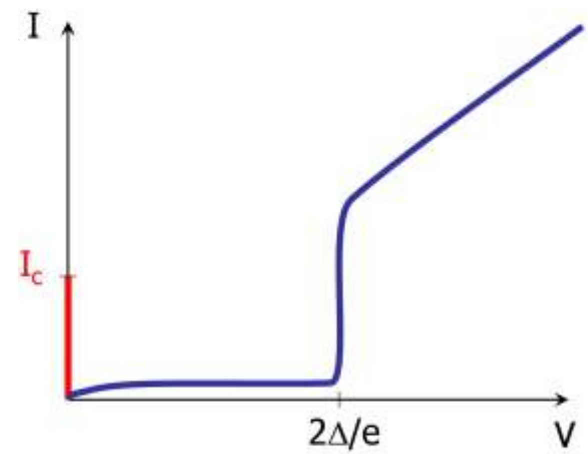

Nonlinear IVC
→ Mixers up to THz, oscillators

Macroscopic quantum behavior
→ Superconducting qubits (ch. 6)

Superconducting Quantum Interference Devices (SQUID)

Single Josephson junction = Magnetic field sensor

$$I_s^m = I_s^m(B)$$

→ Sensitivity: $\frac{dI_s}{dB} = \frac{dI_s}{d\Phi} t_B L \approx \frac{I_s^m}{\Phi_0} t_B L$

→ Increase area $A = t_B L$ to increase sensitivity

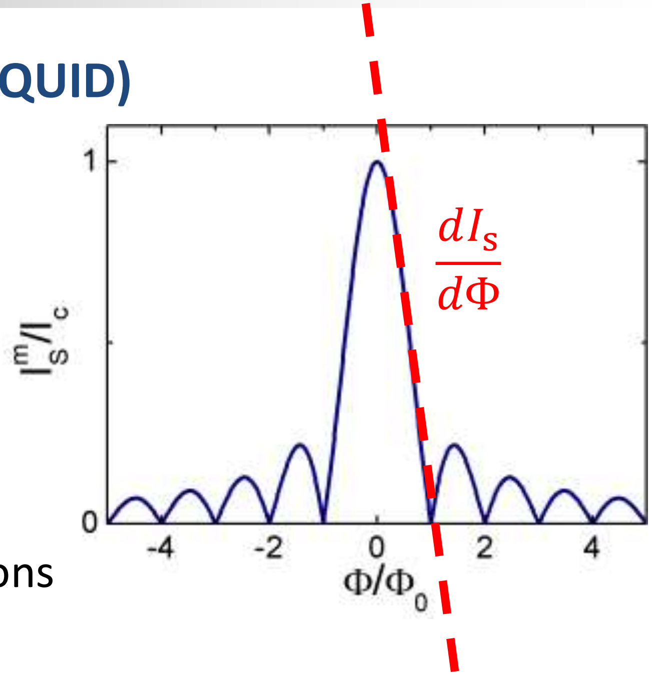

Superconducting loop with one or more Josephson junctions

→ Relevant area = Loop area

→ Dual- or multi-beam interference

Superconducting Quantum Interference Devices (SQUIDs)

→ Relevant physics: flux quantization & Josephson effect

→ Most sensitive detectors for magnetic flux

→ Can detect any quantity that can be converted into magnetic flux: magnetic field, field gradient, current, voltage, displacement, …

→ Two important types: Direct current (dc) and radio frequency (rf) SQUIDs

→ Dc-SQUIDs: highest energy sensitivity at low temperatures

4.1 The dc SQUID

Definition

→ Parallel circuit of two lumped elements Josephson junctions

→ Important for sensing applications

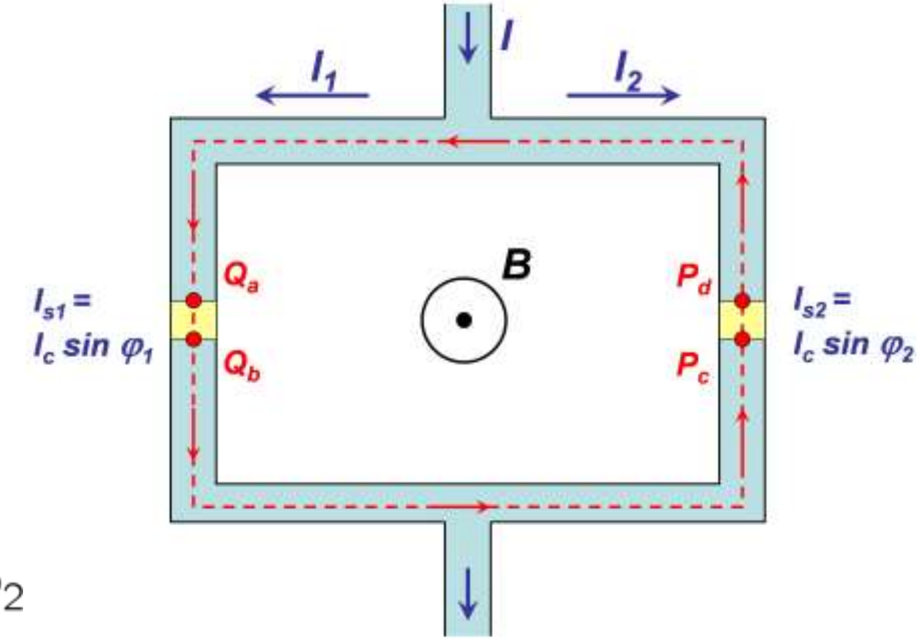

Simplification

→ Identical I_c (symmetric dc SQUID)

$$I_s = I_{s1} + I_{s2} = I_c \sin\varphi_1 + I_c \sin\varphi_2$$

$$= 2I_c \cos\left(\frac{\varphi_1 - \varphi_2}{2}\right) \sin\left(\frac{\varphi_1 + \varphi_2}{2}\right)$$

4.1.1 The zero voltage state

Total phase change along closed contour = 2πn:

$$\oint_C \nabla\theta \cdot d\mathbf{l} = 2\pi n$$

$$= (\theta_{Q_b} - \theta_{Q_a}) + (\theta_{P_c} - \theta_{Q_b}) + (\theta_{P_d} - \theta_{P_c}) + (\theta_{Q_a} - \theta_{P_d})$$

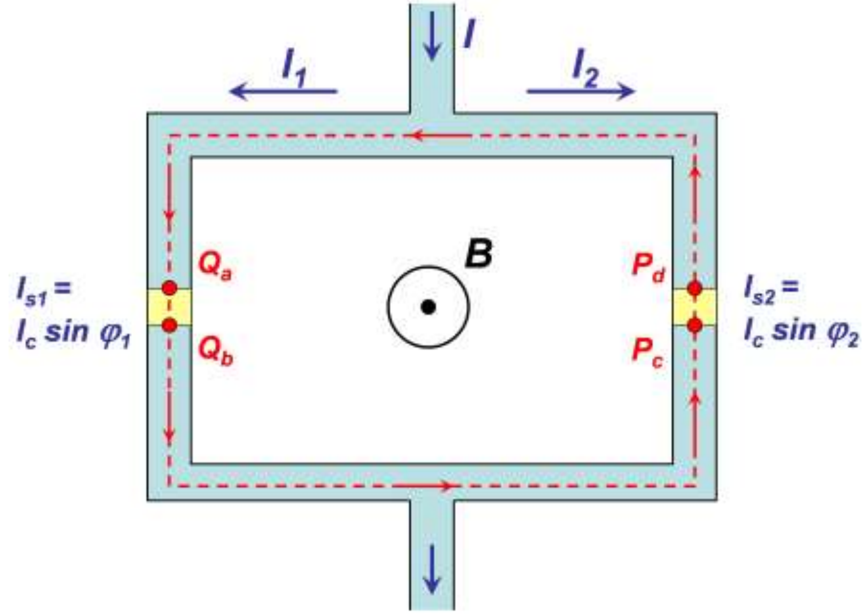

$$\nabla\theta = \frac{2\pi}{\Phi_0}(\Lambda \mathbf{J}_s + \mathbf{A})$$

$$\varphi = \theta_2 - \theta_1 - \frac{2\pi}{\Phi_0}\int_1^2 \mathbf{A}\cdot d\mathbf{l}$$

$$\theta_{Q_b} - \theta_{Q_a} = +\varphi_1 + \frac{2\pi}{\Phi_0}\int_{Q_a}^{Q_b} \mathbf{A}\cdot d\mathbf{l}$$

$$\theta_{P_d} - \theta_{P_c} = -\varphi_2 + \frac{2\pi}{\Phi_0}\int_{P_c}^{P_d} \mathbf{A}\cdot d\mathbf{l}$$

$$\theta_{P_c} - \theta_{Q_b} = \int_{Q_b}^{P_c} \nabla\theta \cdot d\ell = +\frac{2\pi}{\Phi_0}\int_{Q_b}^{P_c} \Lambda\mathbf{J}_s \cdot d\mathbf{l} + \frac{2\pi}{\Phi_0}\int_{Q_b}^{P_c} \mathbf{A}\cdot d\mathbf{l}$$

$$\theta_{Q_a} - \theta_{P_d} = \int_{P_d}^{Q_a} \nabla\theta \cdot d\ell = +\frac{2\pi}{\Phi_0}\int_{P_d}^{Q_a} \Lambda\mathbf{J}_s \cdot d\mathbf{l} + \frac{2\pi}{\Phi_0}\int_{P_d}^{Q_a} \mathbf{A}\cdot d\mathbf{l}$$

4.1.1 The zero voltage state

Substitution → $\varphi_1 - \varphi_2 = -\frac{2\pi}{\Phi_0}\oint_C \mathbf{A}\cdot d\ell - \frac{2\pi}{\Phi_0}\int_{Q_b}^{P_c} \Lambda \mathbf{J}_s \cdot d\ell - \frac{2\pi}{\Phi_0}\int_{P_d}^{Q_a} \Lambda \mathbf{J}_s \cdot d\ell$

Integrate vector potential $\boldsymbol{A}$

Closed loop → Total flux Φ threading the loop

Integrate self-induced current $\boldsymbol{J}_s$

$\boldsymbol{J}_s$ vanishes deep inside electrode material → $\int \Lambda \boldsymbol{J}_s \cdot d\ell$ vanishes

→ Phase differences are not independent but linked via the fluxoid quantization

$$\varphi_2 - \varphi_1 = \frac{2\pi\Phi}{\Phi_0}$$

$$I_s = 2I_c \cos\left(\frac{\varphi_1 - \varphi_2}{2}\right)\sin\left(\frac{\varphi_1 + \varphi_2}{2}\right)$$

$$\Rightarrow I_s = 2I_c \cos\left(\pi\frac{\Phi}{\Phi_0}\right)\sin\left(\varphi_1 + \pi\frac{\Phi}{\Phi_0}\right)$$

$\Phi = \Phi_{\text{ext}}$ → Maximum supercurrent is obtained for $\sin\left(\varphi_1 + \pi\frac{\Phi}{\Phi_0}\right) = 1$

$$\boxed{I_s^m = 2I_c \left|\cos\left(\pi\frac{\Phi_{\text{ext}}}{\Phi_0}\right)\right|}$$

4.1.1 The zero voltage state

In reality often finite inductance L of the loop → Total flux $\Phi = \Phi_{\mathrm{ext}} + \Phi_L$

Intuitive variables (symmetric loop)

$$I_{s1} = \widetilde{I} + I_{\mathrm{cir}} \qquad \widetilde{I} = (I_{s1} + I_{s2})/2$$ Average (transport) supercurrent

$$I_{s2} = \widetilde{I} - I_{\mathrm{cir}} \qquad I_{\mathrm{cir}} = (I_{s1} - I_{s2})/2$$ Circulating current

$$\Rightarrow \Phi = \Phi_{\mathrm{ext}} + L I_{\mathrm{cir}} = \Phi_{\mathrm{ext}} + \frac{L I_c}{2}(\sin\varphi_1 - \sin\varphi_2)$$

$$= \Phi_{\mathrm{ext}} + L I_c \sin\left(\frac{\varphi_1 - \varphi_2}{2}\right)\cos\left(\frac{\varphi_1 + \varphi_2}{2}\right)$$

$$\varphi_2 - \varphi_1 = \frac{2\pi\Phi}{\Phi_0}$$

$$\boxed{\Phi = \Phi_{\mathrm{ext}} - L I_c \sin\left(\pi\frac{\Phi}{\Phi_0}\right)\cos\left(\varphi_1 + \pi\frac{\Phi}{\Phi_0}\right)}$$

$$\boxed{I_s = 2 I_c \cos\left(\pi\frac{\Phi}{\Phi_0}\right)\sin\left(\varphi_1 + \pi\frac{\Phi}{\Phi_0}\right)}$$

Equations have to be solved self-consistently
Maximize I_s with respect to φ_1 with constraint → I_s^{m}

Relevance of finite inductance is characterized by

Screening parameter $\boxed{\beta_L \equiv \frac{2LI_c}{\Phi_0}}$

Negligible screening: $\boldsymbol{\beta_L \ll 1}$

→ Flux due to circulating current can be neglected

→ Maximum supercurrent for given Φ_{ext} requires $\frac{dI_s}{d\varphi_1} = 0$ → $\cos\left(\varphi_1 + \pi\frac{\Phi_{\mathrm{ext}}}{\Phi_0}\right) = 0$

$$\sin\left(\varphi_1 + \pi\frac{\Phi_{\mathrm{ext}}}{\Phi_0}\right) = \pm 1 \quad \Rightarrow I_s^m \simeq 2I_c\left|\cos\left(\pi\frac{\Phi_{\mathrm{ext}}}{\Phi_0}\right)\right|$$

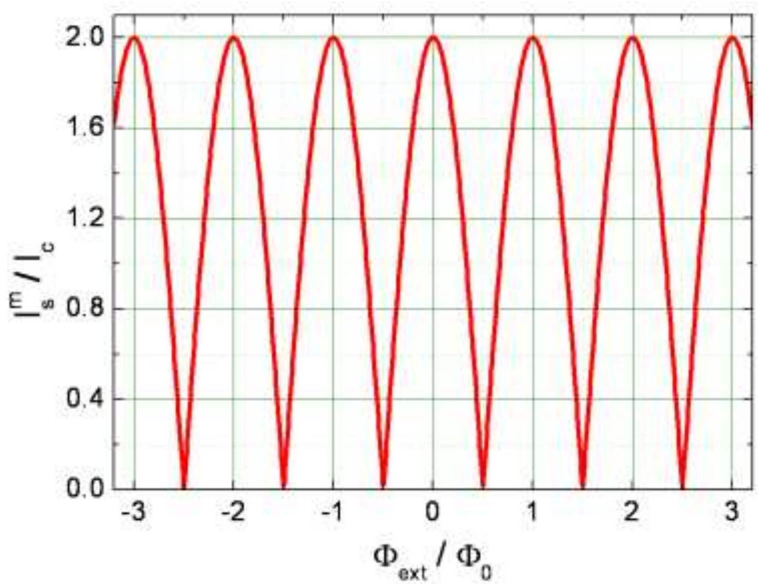

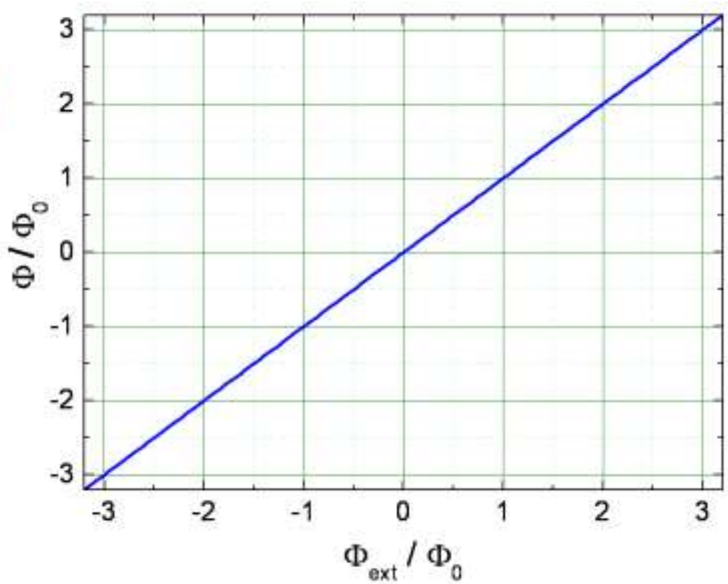

$A = 2\ \mathrm{mm}^2$,
$B_{\mathrm{ext}} = 1\ \mathrm{nT}$
→ $\Phi_{\mathrm{ext}} = \Phi_0$

4.1.1 The zero voltage state

Large screening: $\boldsymbol{\beta_L \gg 1}$

→ $LI_c \gg \Phi_0$ → Circulating current compensates external field

→ Total flux in the loop tends to be quantized

$$\Phi = \Phi_{\mathrm{ext}} + LI_{\mathrm{cir}} \simeq n\Phi_0$$

Example → $I \simeq 0$ → $\sin\varphi_1 \approx -\sin\varphi_2$

$$\Phi_{\mathrm{ext}} = \Phi + LI_c \sin\left(\pi\frac{\Phi}{\Phi_0}\right) \quad \text{or} \quad \frac{\Phi_{\mathrm{ext}}}{\Phi_0} = \frac{\Phi}{\Phi_0} + \frac{\beta_L}{2}\sin\left(\pi\frac{\Phi}{\Phi_0}\right)$$

Finite screening → $\beta_L > 0$

How does $\Phi(\Phi_{\text{ext}})$ look like in detail ?

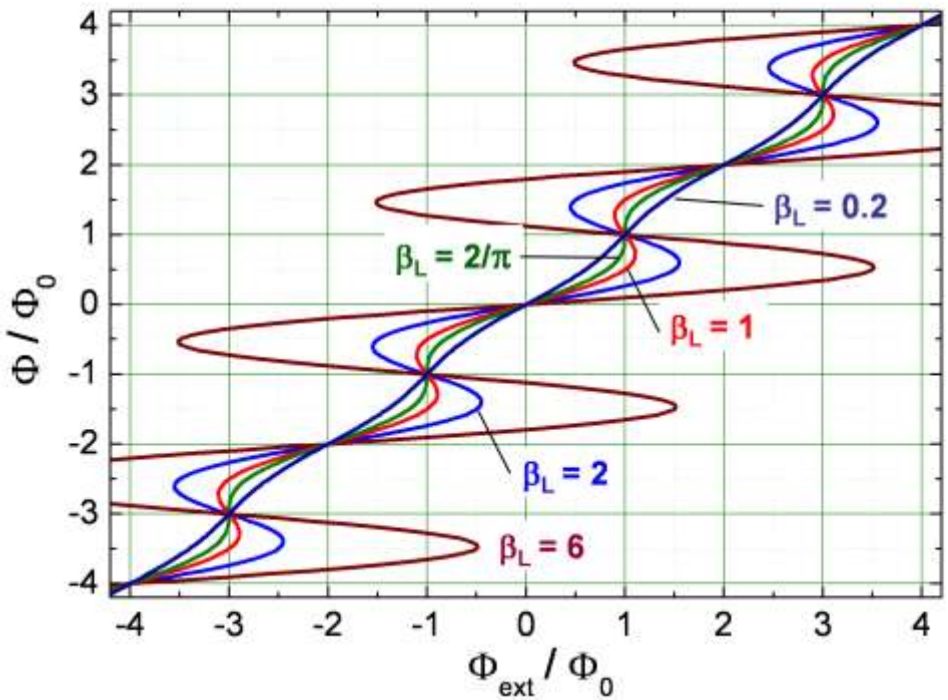

$\Phi(\Phi_{\text{ext}})$ can be single-valued or multiple-valued (hysteretic)

Maximum value of $\Phi_{\text{cir}} \simeq LI_c$

Rough estimate

$\Phi(\Phi_{\text{ext}})$ single valued curve when Φ_{cir} does not bring Φ too far into the next period

$\rightarrow |\Phi_{\text{cir}}| \leq \frac{\Phi_0}{2} \rightarrow LI_c \leq \frac{\Phi_0}{2} \rightarrow \beta_L \leq 1$ (more precisely: $\beta_L \leq \frac{2}{\pi}$)

Dc SQUID response in integer multiples of Φ_0 not affected by screening

4.1.1 The zero voltage state

R. Gross, A. Marx , F. Deppe, and K. Fedorov © Walther-Meißner-Institut (2001 - 2020)

$I_s^{\mathrm{m}}(\Phi_{\mathrm{ext}})$ for large β_L (qualitative discussion)

$$I_{\mathrm{cir}} \simeq -\frac{\Phi_{\mathrm{ext}} - n\Phi_0}{L}$$

$$\Phi = \Phi_{\mathrm{ext}} + L I_{\mathrm{cir}} \simeq n\Phi_0$$

→ $I_{\mathrm{cir}} \to 0$ for large L → $I_s^{\mathrm{m}} \approx 2I_c$

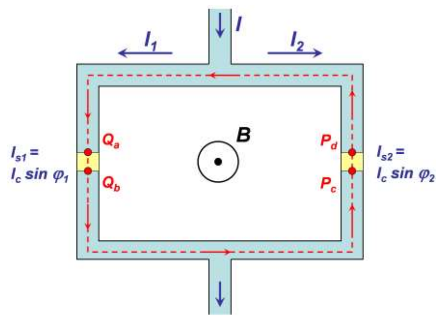

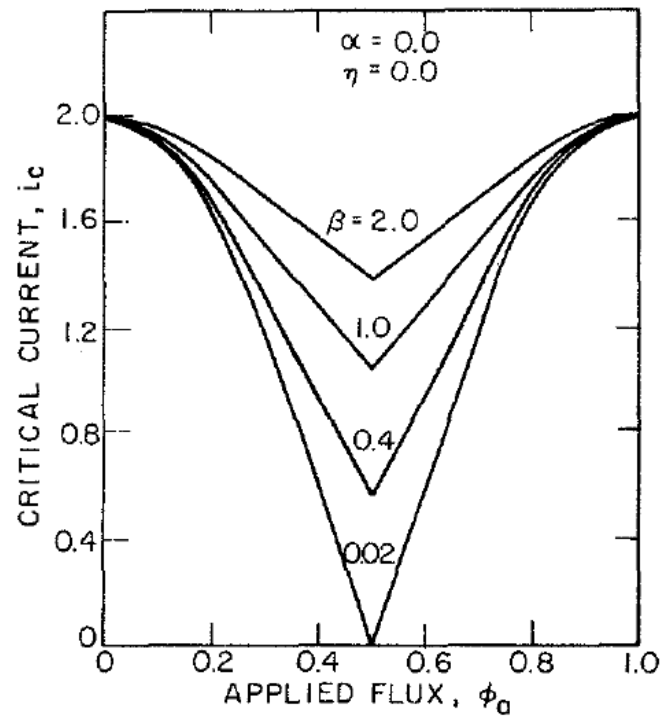

Start with $n = 0$

→ Small screening current $I_{\mathrm{cir}} \approx -\Phi_{\mathrm{ext}}/L$ screens field

→ I_1 decreases, I_2 increases with increasing Φ_{ext} $(I_2 \leq I_c)$

→ At some point I_2 fixed at I_c, then

$$I_1 \simeq I_c - \frac{2\Phi_{\mathrm{ext}}}{L}$$

$$I_{\mathrm{cir}} = (I_{s1} - I_{s2})/2 \qquad \beta_L = \frac{2LI_c}{\Phi_0}$$

$$\Rightarrow I_s^m \simeq 2I_c - \frac{2\Phi_{\mathrm{ext}}}{L} \quad \text{or} \quad \frac{I_s^m}{2I_c} \simeq 1 - \frac{2\Phi_{\mathrm{ext}}}{\Phi_0}\frac{1}{\beta_L}$$

→ Modulation depth of $I_s^{\mathrm{m}}(\Phi_{\mathrm{ext}})$ is strongly reduced with increasing β_L (roughly $\propto 1/\beta_L$)

Negligible screening ($\beta_L \ll 1$) and strong damping ($\beta_C \ll 1$)

→ Total flux = Applied flux
→ (Neglect displacement current)
→ Total current = Josephson current + resistive current

Identical junctions

$$\varphi = \varphi_1 + \pi \frac{\Phi}{\Phi_0}$$

$$\varphi_2 - \varphi_1 = \frac{2\pi\Phi}{\Phi_0}$$

$$\rightarrow I = I_c \sin\varphi_1 + I_c \sin\varphi_2 + \frac{V}{R_N} + \frac{V}{R_N}$$

$$= 2I_c \cos\left(\pi \frac{\Phi}{\Phi_0}\right) \sin\left(\varphi_1 + \pi\frac{\Phi}{\Phi_0}\right) + 2\frac{V}{R_N}$$

Define new phase $\varphi \equiv \varphi_1 + \pi \frac{\Phi}{\Phi_0}$

$$I = 2I_c \cos\left(\pi \frac{\Phi}{\Phi_0}\right) \sin\left(\varphi_1 + \pi\frac{\Phi}{\Phi_0}\right) + 2\frac{V}{R_N}$$

with $\Phi \approx \Phi_{\text{ext}} = const.$ → $\frac{d\varphi}{dt} = \frac{d\varphi_1}{dt} = \frac{2\pi}{\Phi_0} V(t)$

$$\boxed{I = I_s^m(\Phi_0) sin\,\varphi + \frac{2}{R_N}\frac{\Phi_0}{2\pi}\frac{d\varphi}{dt} \quad \text{with} \quad I_s^m(\Phi_{ext}) = 2I_c cos\left(\pi\frac{\Phi_{ext}}{\Phi_0}\right)}$$

→ IVC of single junction with flux dependent $I_c = I_c(\Phi_{\text{ext}})$

Mechanical analog → Two pendula with rigid coupling because of $\beta_L \ll 1$

4.1.2 The voltage state

$$\langle V(t)\rangle = I_c R_N \sqrt{\left(\frac{I}{2I_c}\right)^2 - \left(\frac{I_s^m(\Phi_{\text{ext}})}{2I_c}\right)^2} = I_c R_N \sqrt{\left(\frac{I}{2I_c}\right)^2 - \left[\cos\left(\pi\frac{\Phi_{\text{ext}}}{\Phi_0}\right)\right]^2}$$

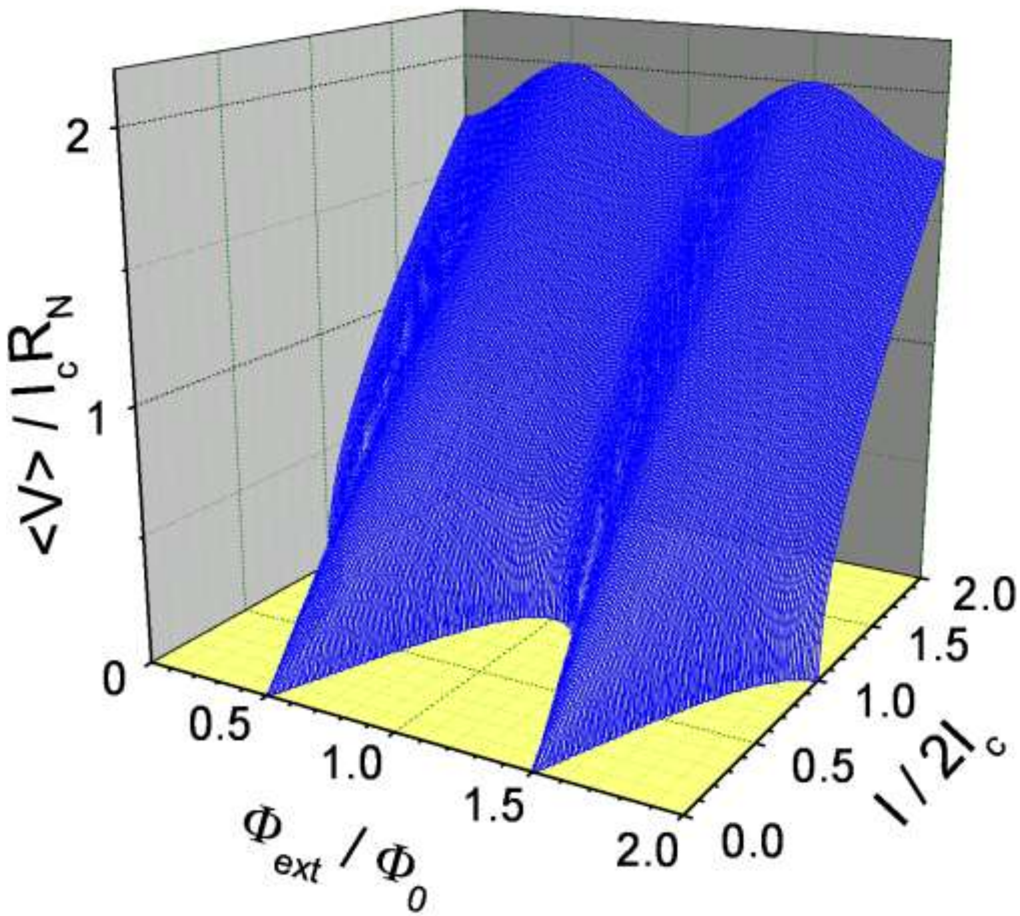

Single junction IVC for $\beta_C \ll 1$

$$\langle V(t)\rangle = I_c R \sqrt{\left(\frac{I}{I_c}\right)^2 - 1}$$

→ Φ_0-periodic IVCs
→ Periodic $\langle V\rangle(\Phi_{\text{ext}})$
→ Minima & maxima at same flux values
→ Maximum modulation for $I \approx 2I_c$

4.1.2 The voltage state

Finite screening: $\beta_L \approx 1$, intermediate damping: $\beta_C \approx 1$

→ Increase flux threading loop → Larger loops → Large L

→ Consider displacement + noise current → Numerical solution required!

Basic equations

$$V = \frac{\Phi_0}{4\pi}\left(\frac{d\varphi_1}{dt} + \frac{d\varphi_2}{dt}\right)$$

Relates voltage to phase change

$$2\pi n = \varphi_2 - \varphi_1 - 2\pi\frac{\Phi_{\mathrm{ext}}}{\Phi_0} - 2\pi\frac{L I_{\mathrm{cir}}}{\Phi_0}$$

Fluxoid quantization

$$\frac{I}{2} = \frac{\hbar C}{2e}\frac{d^2\varphi_1}{dt^2} + \frac{\hbar}{2eR_N}\frac{d\varphi_1}{dt} + [I_c \sin\varphi_1 + I_{\mathrm{cir}}] + I_{F1}$$

coupling

$$\frac{I}{2} = \frac{\hbar C}{2e}\frac{d^2\varphi_2}{dt^2} + \frac{\hbar}{2eR_N}\frac{d\varphi_2}{dt} + [I_c \sin\varphi_2 - I_{\mathrm{cir}}] + I_{F2}$$

Mechanical analog

→ Two pendula with mass M and length ℓ coupled via twistable bar

→ Negligible screening ($\beta_L \ll 1$)

- → Rigid bar
- → Relative angle $\varphi_1 - \varphi_2 = 2\pi \frac{\Phi_{\text{ext}}}{\Phi_0}$ fixed by external flux
- → Single pendulum with mass 2M
- → Distance from pivot point $I \cos\left(\frac{\varphi_1 - \varphi_2}{2}\right)$
- → Zero torque → Pendula reside at $\frac{\varphi_1 - \varphi_2}{2}$
- → Finite torque (bias current) → Pendulum rotates

→ Finite screening

- → Relative motion of the pendula
- → Coupling → Numerical solution

$I = 0$

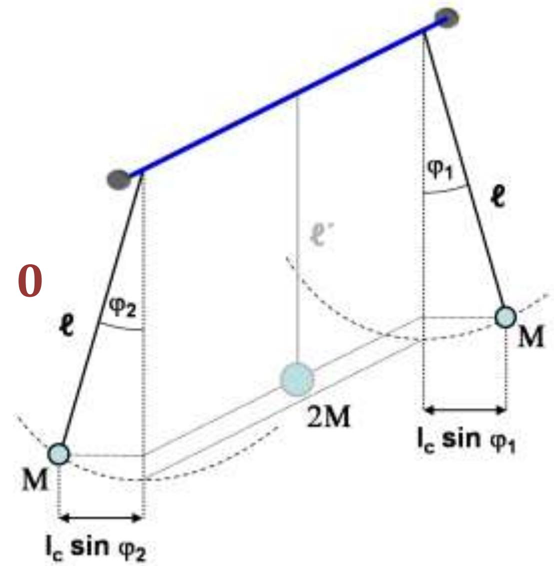

$I > 0$

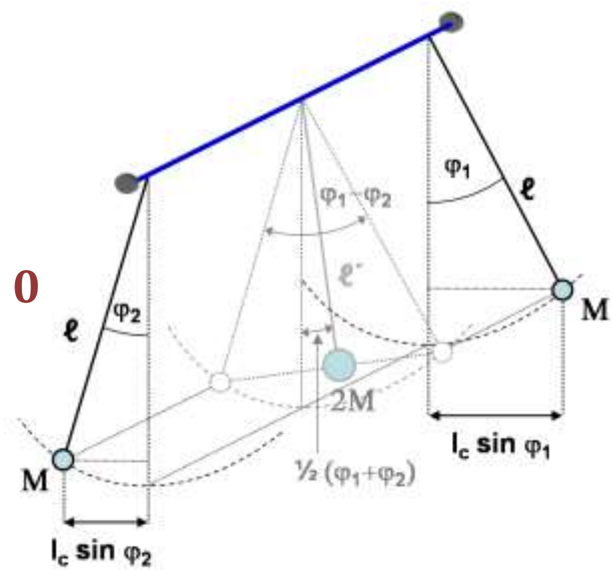

4.1.3 Operation and performance of dc SQUIDs

$\beta_C < 1 \rightarrow$ Non-hysteretic IVCs

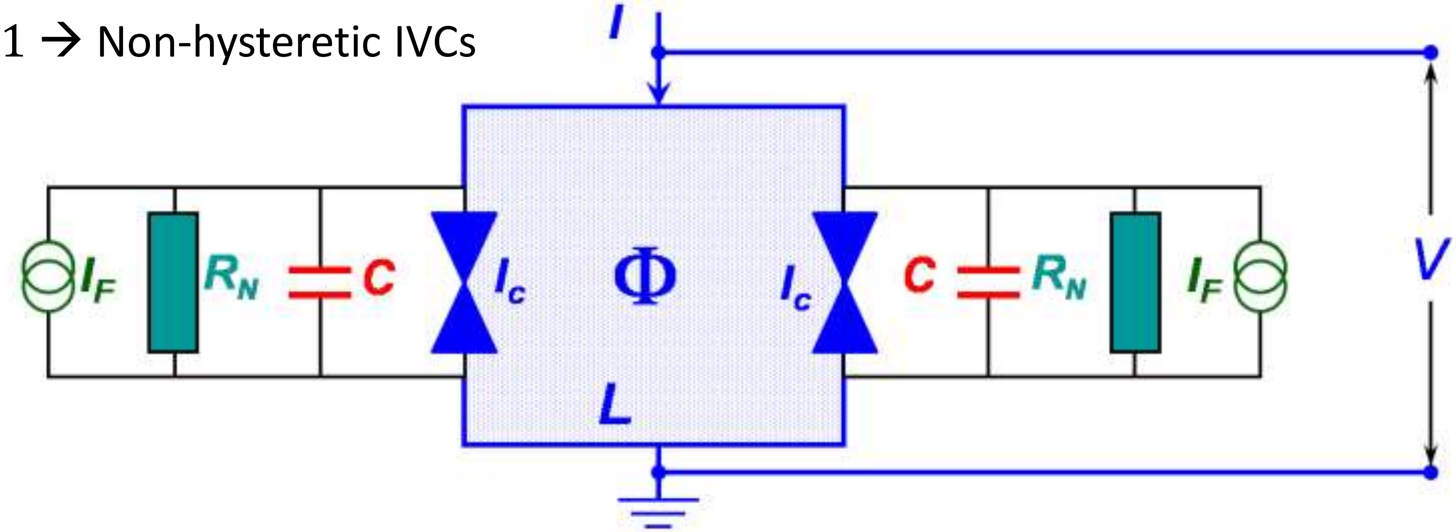

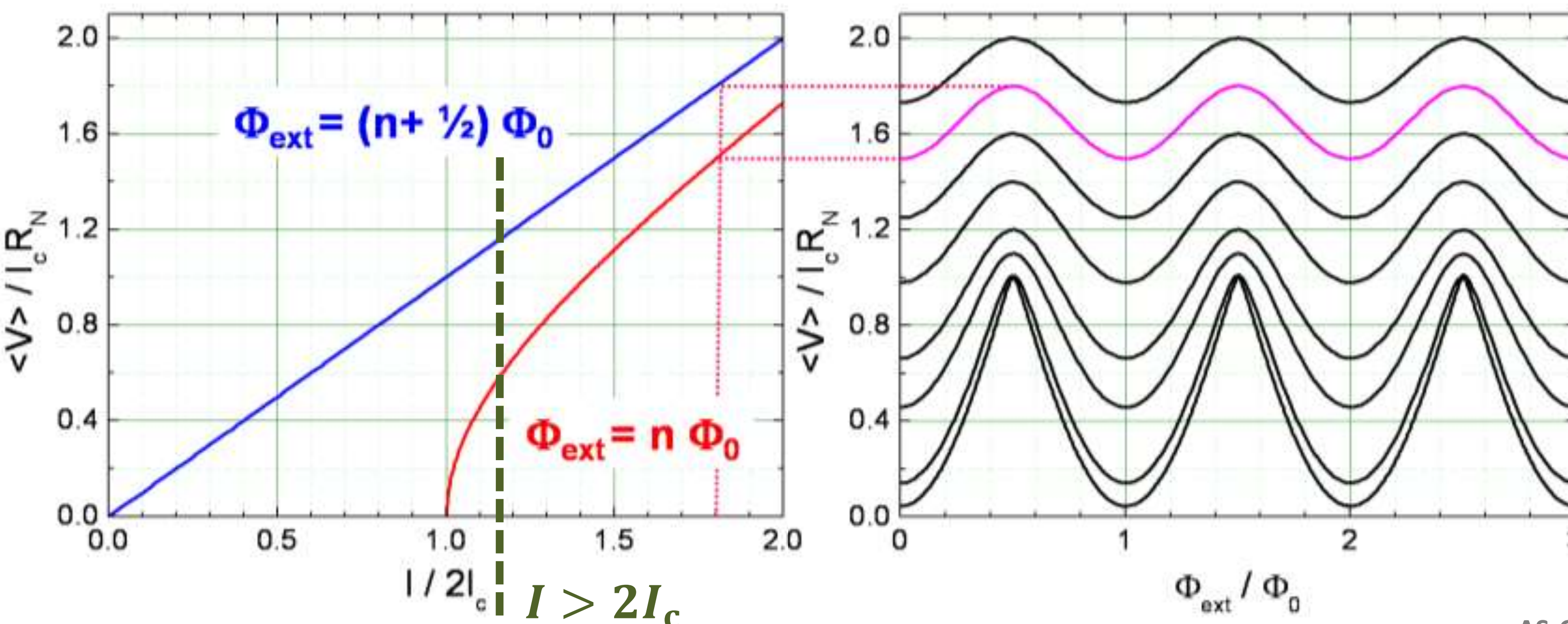

$\beta_C < 1 \rightarrow$ Non-hysteretic IVCs

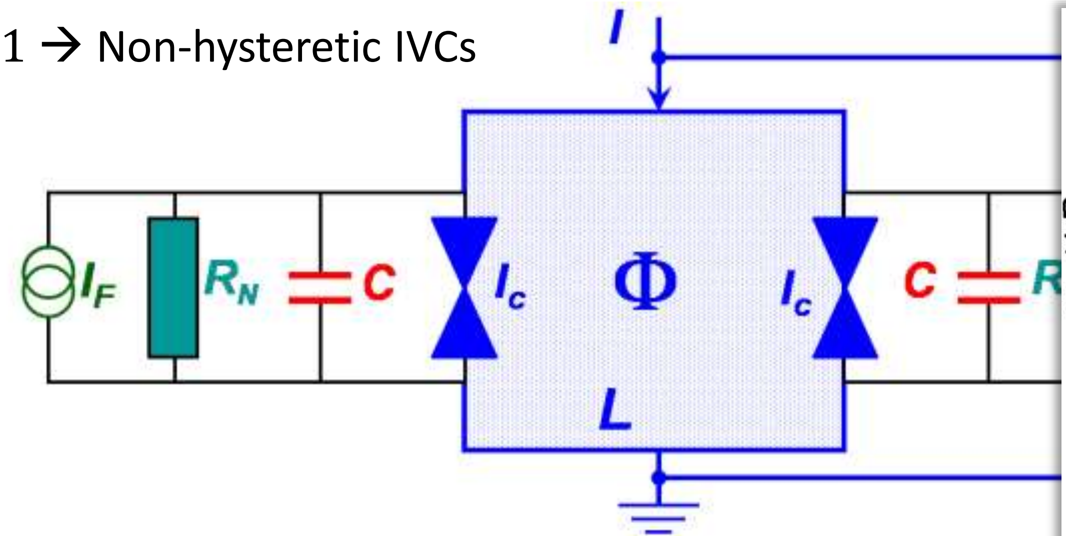

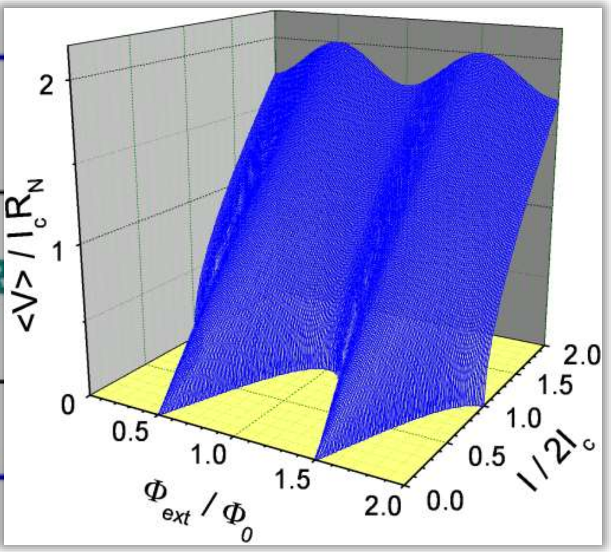

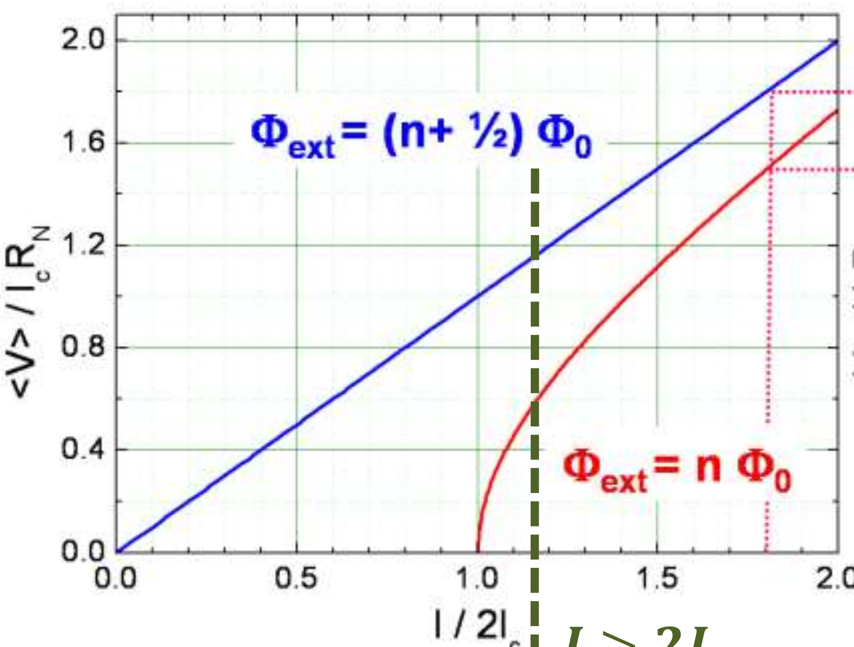

$I > 2I_c$

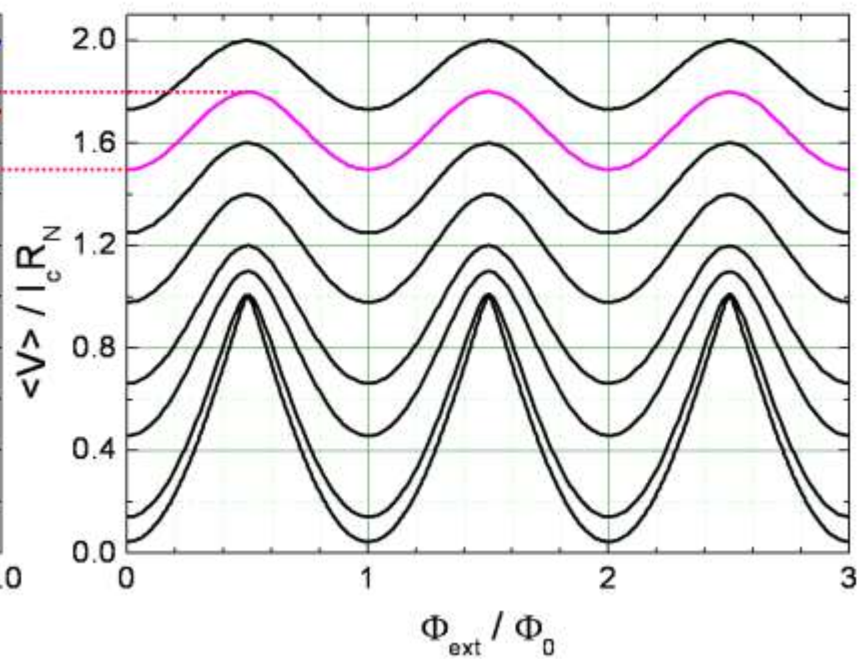

4.1.3 Operation and performance of dc SQUIDs

Important parameters for practical applications of SQUIDs

Main goal → High resolution = Low noise!

Flux-to-voltage transfer coefficient (measure of sensitivity to flux):

$$H \equiv \left| \left(\frac{\partial V}{\partial \Phi_{\text{ext}}} \right)_{I=const} \right|$$

Maximum at steepest point of $\langle V \rangle(\Phi_{\text{ext}})$
→ Flux to voltage transducer

Equivalent flux noise (measure of flux resolution)

$$S_\Phi(f) = \frac{S_V(f)}{H^2}$$

$S_V(f)$ = Power spectral density of voltage noise at fixed bias current

Noise energy (measure of energy resolution when comparing different geometries)

$$\epsilon(f) = \frac{S_\Phi(f)}{2L} = \frac{S_V(f)}{2LH^2}$$

Sets energy resolution
Should be as small as possible!

4.1.3 Operation and performance of dc SQUIDs

Of course it is always good to reduce the noise itself, but typically $S_V(f)$ given → Maximize H and L!

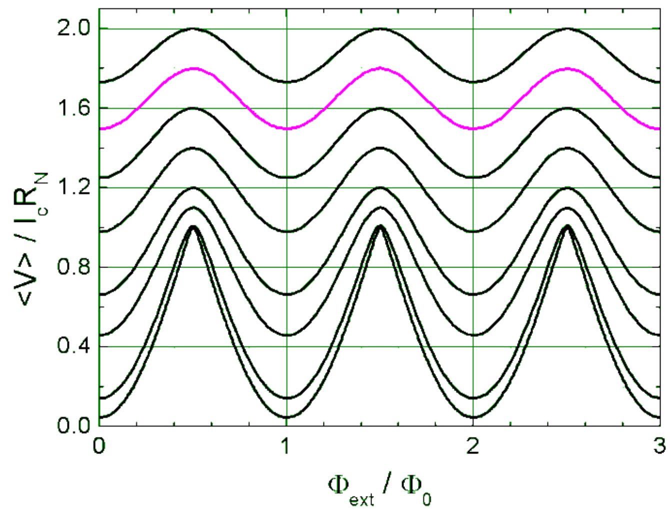

1. Current & flux bias
   - $I \approx I_c, \Phi_{\mathrm{ext}} \approx \frac{2n+1}{4}\Phi_0$
   - Largest modulation of $\langle V\rangle(\Phi_{\mathrm{ext}})$
2. Junction critical current
   - Coupling energy $E_{\mathrm{J}} \gg k_{\mathrm{B}}T$
   - Simulations → $\frac{1}{5}I_{\mathrm{c}} \gtrsim I_{\mathrm{th}} = \frac{2\pi k_{\mathrm{B}}T}{\Phi_0}$
   - $T = 4.2\ \mathrm{K}$ → $I_{\mathrm{c}} \gtrsim 1\ \mu\mathrm{A}$
3. Loop inductance
   - Should be large, but thermal flux noise $\sqrt{k_B T L}$ should be $\ll \Phi_0$
   - Define thermal inductance $L_{\mathrm{th}}I_{\mathrm{th}} \equiv \frac{\Phi_0}{2}$
   - Simulations → $5L \lesssim L_{\mathrm{th}}$ → $L \lesssim 1\ \mathrm{nH}$ @ 4.2K

   - Define $\beta_{\mathrm{th}} \equiv \frac{2I_{\mathrm{th}}L}{\Phi_0} = \frac{L}{L_{\mathrm{th}}} = \frac{I_{\mathrm{th}}}{I_{\mathrm{c}}}\beta_L \lesssim 0.2$

4.1.3 Operation and performance of dc SQUIDs

$S_V(f)$ given → Maximize H and L!

4. Screening parameter
   - $\beta_L = \frac{2 I_c L}{\Phi_0}$
   - No hysteresis in $\langle V \rangle(\Phi_{\mathrm{ext}})$
   - Small L, but large area → Choose $\beta_L \approx 1$
   - Smallest possible $I_c \approx 1\ \mu\mathrm{A}$ @ 4.2 K → $L \approx 1\ \mathrm{nH}$
   - Does not contradict 3
5. Stewart-McCumber parameter
   - No hysteresis in IVC → $\beta_C \leq 1$
   - Underdamped junctions → Shunt resistor
   - Choose $\beta_C \approx 1$ for large voltage output

4.1.3 Operation and performance of dc SQUIDs

Detailed numerical simulations

→ $\epsilon(f)$ minimum for $\beta_L \simeq 1$, $\beta_C \simeq 1$ at $(2n+1)\frac{\Phi_0}{4}$ for max. voltage modulation ($\approx I_c R_N$)

then

$$H = \left| \left(\frac{\partial V}{\partial \Phi_{\text{ext}}} \right)_{I=const} \right| \simeq \frac{I_c R_N}{\Phi_0/2} \simeq \frac{R_N}{L}$$

$$S_I^{in} = 4k_B T/(R_N/2)$$

In-phase current fluctuations

$$S_I^{out} = 4k_B T/2R_N$$

Out-of-phase current fluctuations

Small signal analysis in white noise regime (@ optimal point)

$$S_V(f) = S_I^{in}(f)R_d^2 + S_I^{out}(f)L^2\,H^2 = \frac{4k_B T}{R_N}\left[2R_d^2 + \frac{L^2H^2}{2}\right] \simeq 18 k_B T R_N$$

R_d = differential resistance at the operation point

$$\Rightarrow \epsilon(f) = \frac{S_V(f)}{2LH^2} \simeq \frac{9k_B T L}{R_N} \simeq \frac{9k_B T \Phi_0}{2I_c R_N} \quad \text{for } \beta_L \simeq 1$$

$\beta_L = 2I_c L/\Phi_0 \simeq 1$

$\beta_C = 2\pi I_c R_N^2 C/\Phi_0 \simeq 1$

$$\Rightarrow \epsilon(f) \simeq 16 k_B T \sqrt{\frac{LC}{\beta_C}} \simeq 16\sqrt{\pi} k_B T \sqrt{\frac{\Phi_0 C_s}{2\pi J_c}} = \frac{16\sqrt{\pi} k_B T}{\omega_p} \quad \text{for } \beta_L \simeq 1;\ \beta_C \simeq 1$$

→ **Miminize T, C and maximize J_c, ω_p**

4.1.3 Operation and performance of dc SQUIDs

Improve performance of dc-SQUID

→ Decrease T and C, increase J_c
→ $\epsilon(f)$ is given in units of $\hbar \simeq 10^{-34}$ Js
→ Optimized SQUIDs approach quantum limit $\hbar/2$
→ Practical SQUIDs: $\epsilon(f) \approx 10\hbar$

Dimensionless parameter
$$\beta_{\mathrm{th}} = \gamma\beta_L = \frac{2\pi k_B T}{I_c\Phi_0}\frac{2I_cL}{\Phi_0} = \frac{L}{\frac{\Phi_0^2}{4\pi k_B T}} \equiv \frac{L}{L_{\mathrm{th}}}$$

Reduced noise energy

$$\Sigma(f) = \frac{\epsilon(f)}{\frac{2\Phi_0 k_B T}{I_c R_N}}$$

Rapid increase for $\gamma\beta_L > 0.2$
→ Due to thermal noise rounding of IVC
→ Corresponds to $L \lesssim \frac{1}{5}L_{\mathrm{th}}$

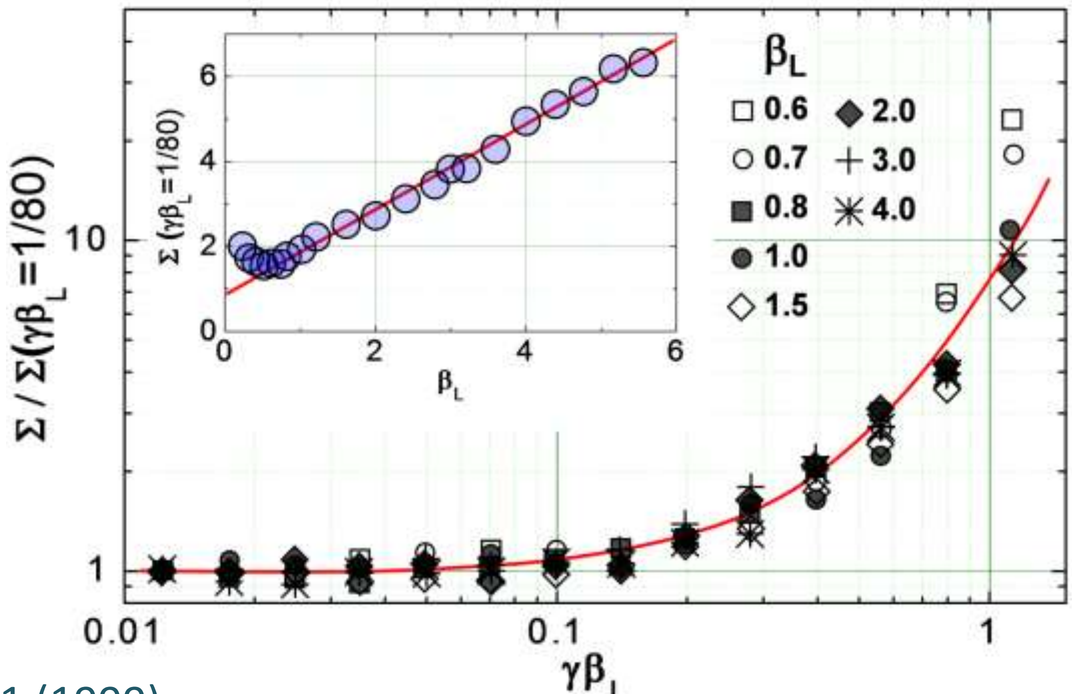

D. Kölle et al., Rev. Mod. Phys. **71**, 631 (1999)

4.1.4 Practical dc-SQUIDs

Required components

→ Antenna
→ SQUID (cryogenic)
→ Room temperature electronics

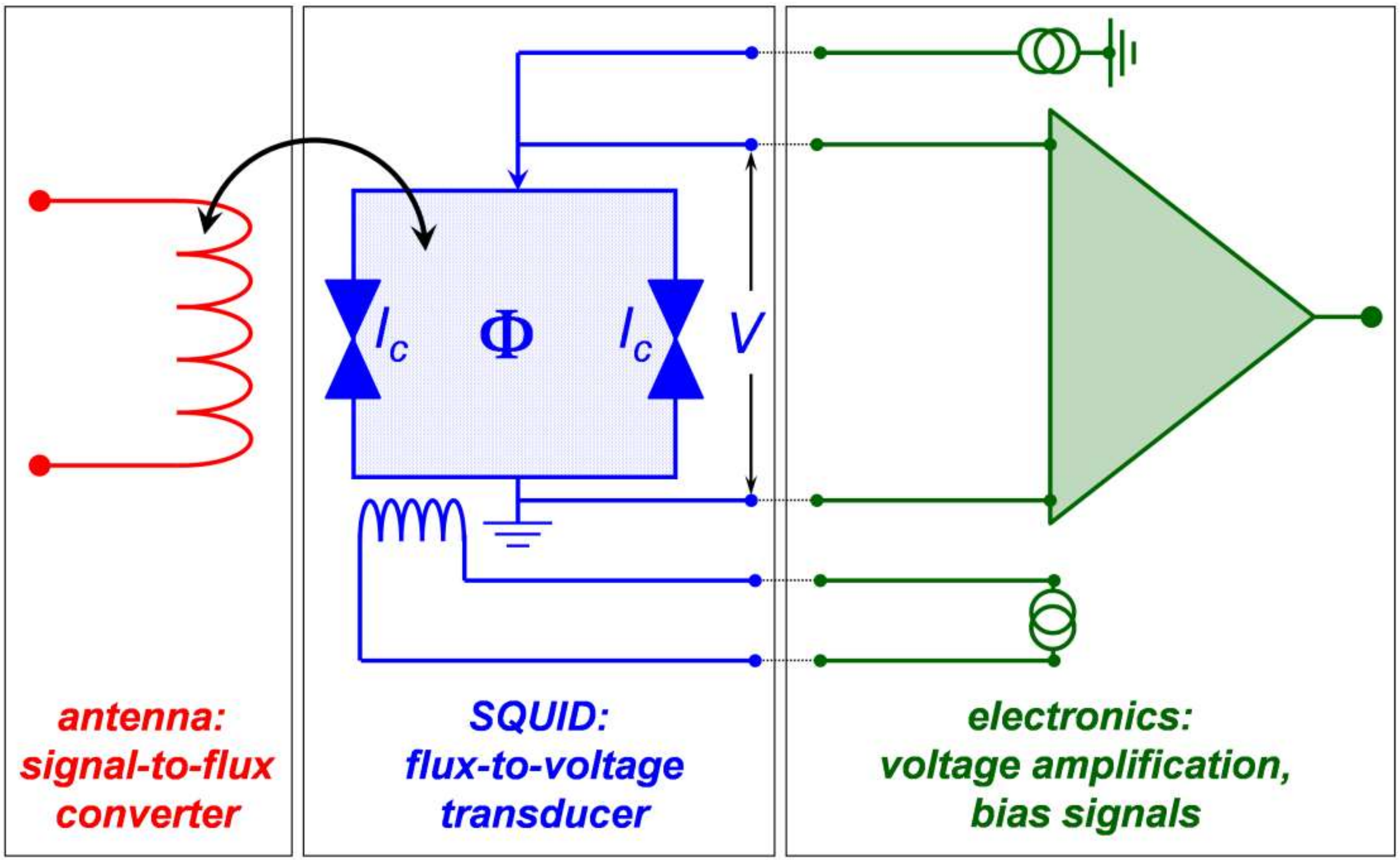

SQUID geometries

Today's SQUIDs and antenna consist of **thin film structures**
→ Fabrication by optical and electron beam lithography

→ Requirements
- → Large sensitivity → Large area A → Large L
- → Deterioration of performance

$$\Delta\Phi_{\mathrm{ext}} = A \cdot \Delta B$$

Washer type SQUID

→ Large effective area and small inductance (perfect diamagnetism)

→ Easy coupling to antenna via planar spiral coil

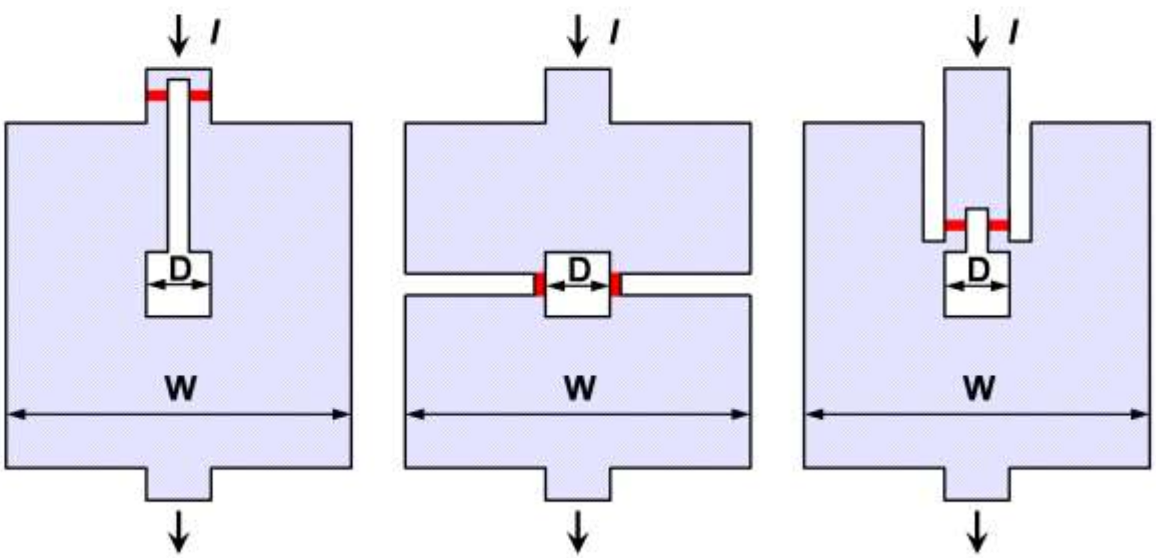

Loop currents around inner opening → $L = 1.25\mu_0 D$ (for $W \gg D$)

→ Effective area: $A_{\mathrm{eff}} \propto D \times W$

Limit: flux trapping in washer area → Flux noise by thermally activated motion

Flux focusing effect in washer-type YBCO grain boundary junction dc SQUID

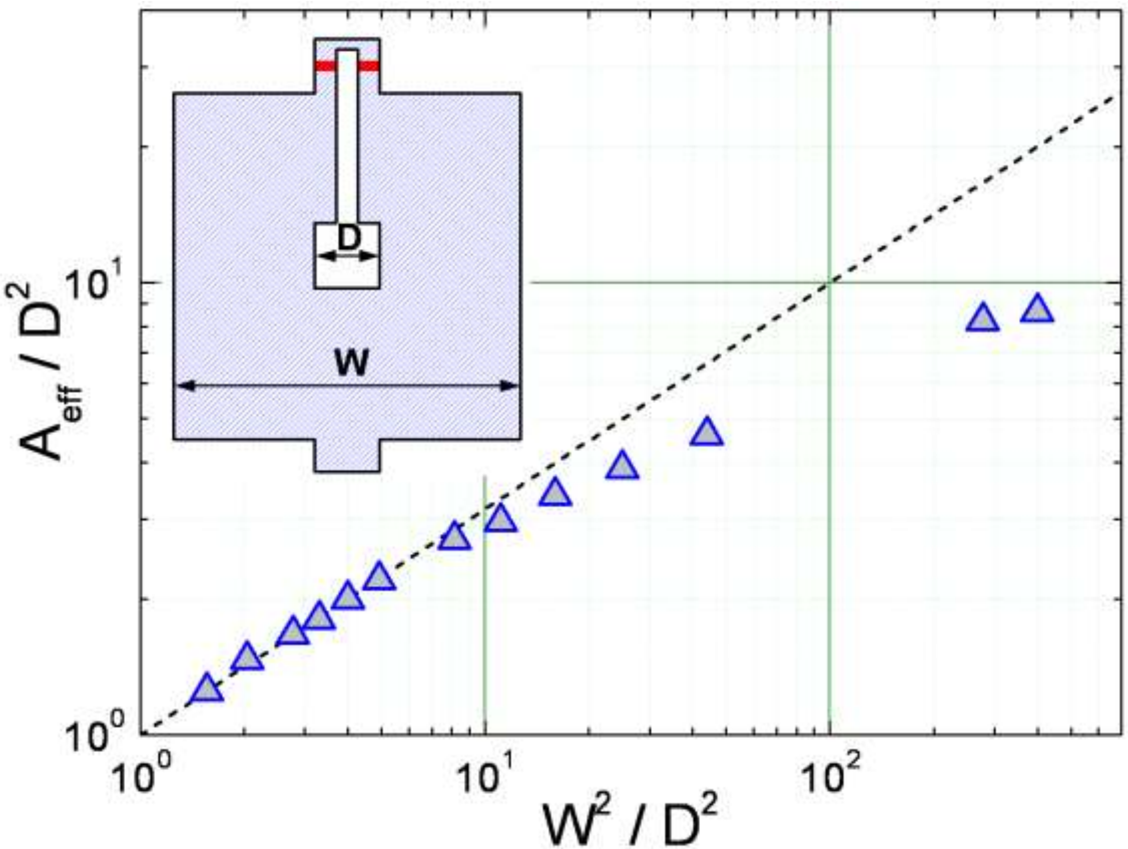

M.B. Ketchen et al.,
Appl. Phys. Lett. **40**, 736 (1982)

R. Gross et al.,
Appl. Phys. Lett. **57**, 727 (1990)

4.1.4 Practical dc-SQUIDs

Spiral input coil

Coil inductance:

$$L_i \simeq n^2 L + L_s$$

Mutual inductance
(ideal coil-SQUID coupling)

$$M_i \simeq \sqrt{n^2 L \cdot L} = nL$$

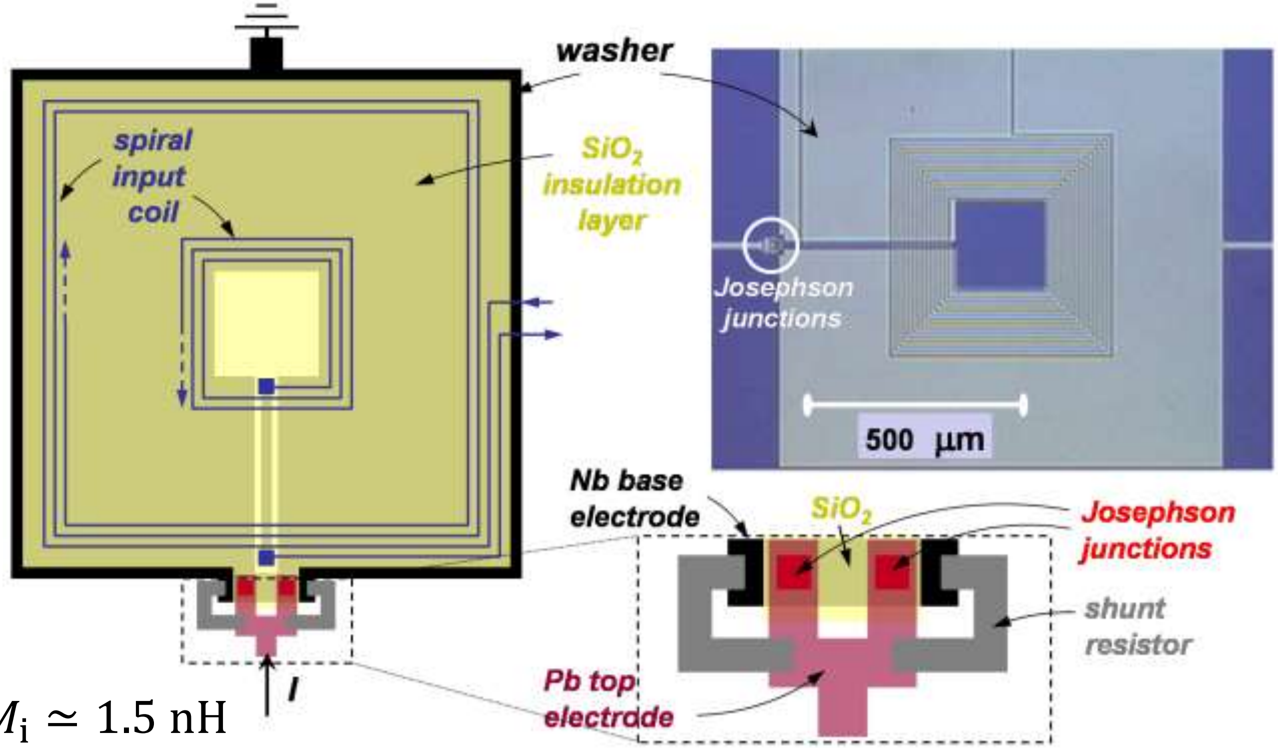

Example

$D = 20\ \mu\text{m} \rightarrow L \simeq 30\ \text{pH}$
$n = 50 \rightarrow L_\text{i} \simeq 75\ \text{nH}$ and $M_\text{i} \simeq 1.5\ \text{nH}$

Real devices → Coupling coefficient $\alpha \equiv \frac{M_\text{i}}{\sqrt{L_\text{i} L}}$

$$\alpha^2 \simeq \frac{1}{1 + L_s / n^2 L} \qquad (\alpha_\text{exp} \simeq 0.6 - 0.8)$$

$L_\text{s} =$ Stripline inductance
$n =$ # of turns
$n^2 L =$ coil geometric self inductance

$$\alpha = M_i / \sqrt{L_i L} = nL / \sqrt{(n^2 L + L_s) L}$$

Specific problem: Capacitance between spiral input coil and square washer
→ LC resonances → Excess noise

4.1.4 Practical dc-SQUIDs

Low-T_c dc SQUIDs

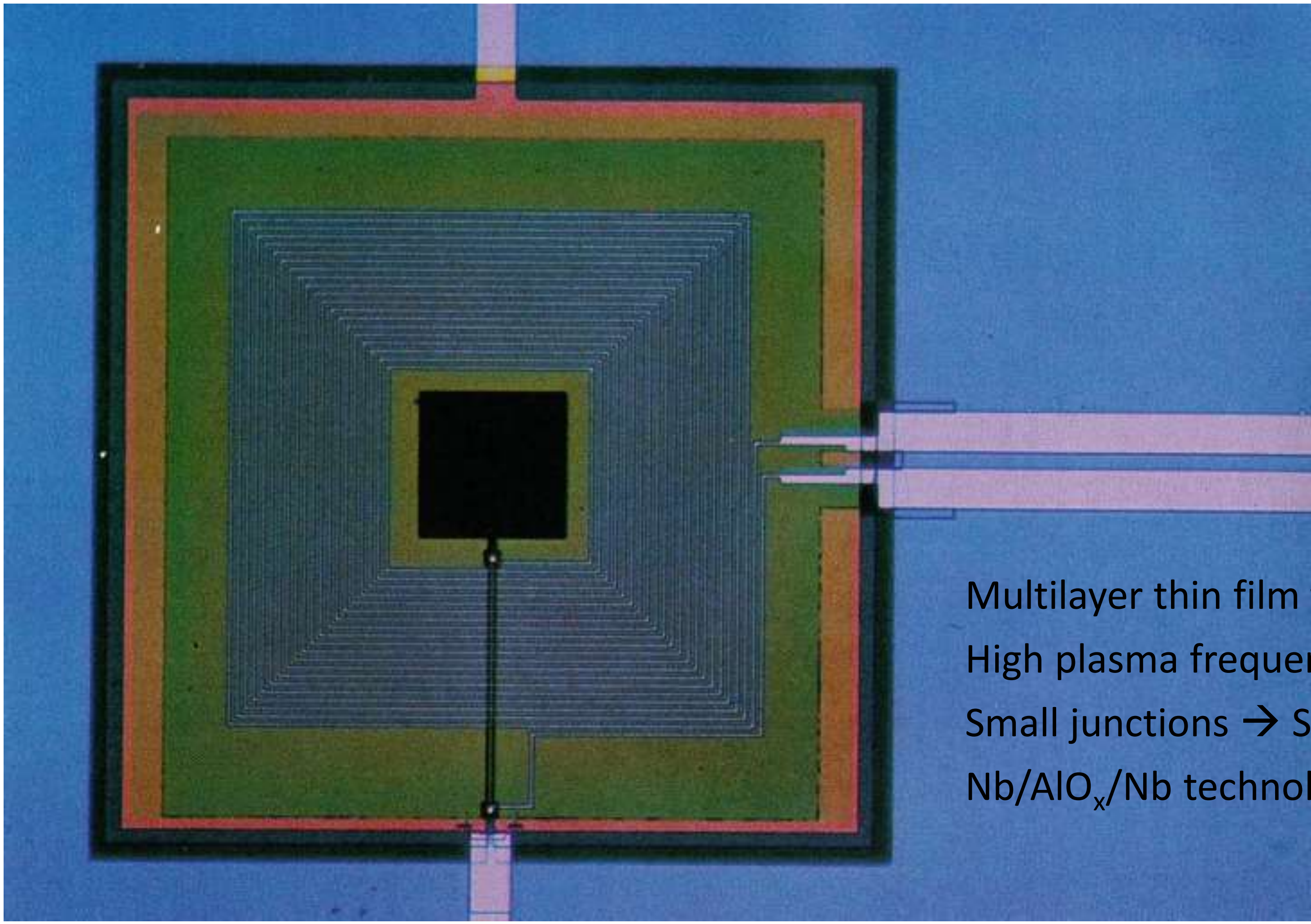

Multilayer thin film technology

High plasma frequency (high J_c)

Small junctions → Small capacitance

Nb/AlO_x/Nb technology

4.1.4 Practical dc-SQUIDs

High-T_c dc SQUIDs

→ Heteroepitaxial growth of the different SC layers
→ Low reproducibility of junctions
→ Alternatives: flip-chip design, directly coupled SQUID (only 1 SC layer required)

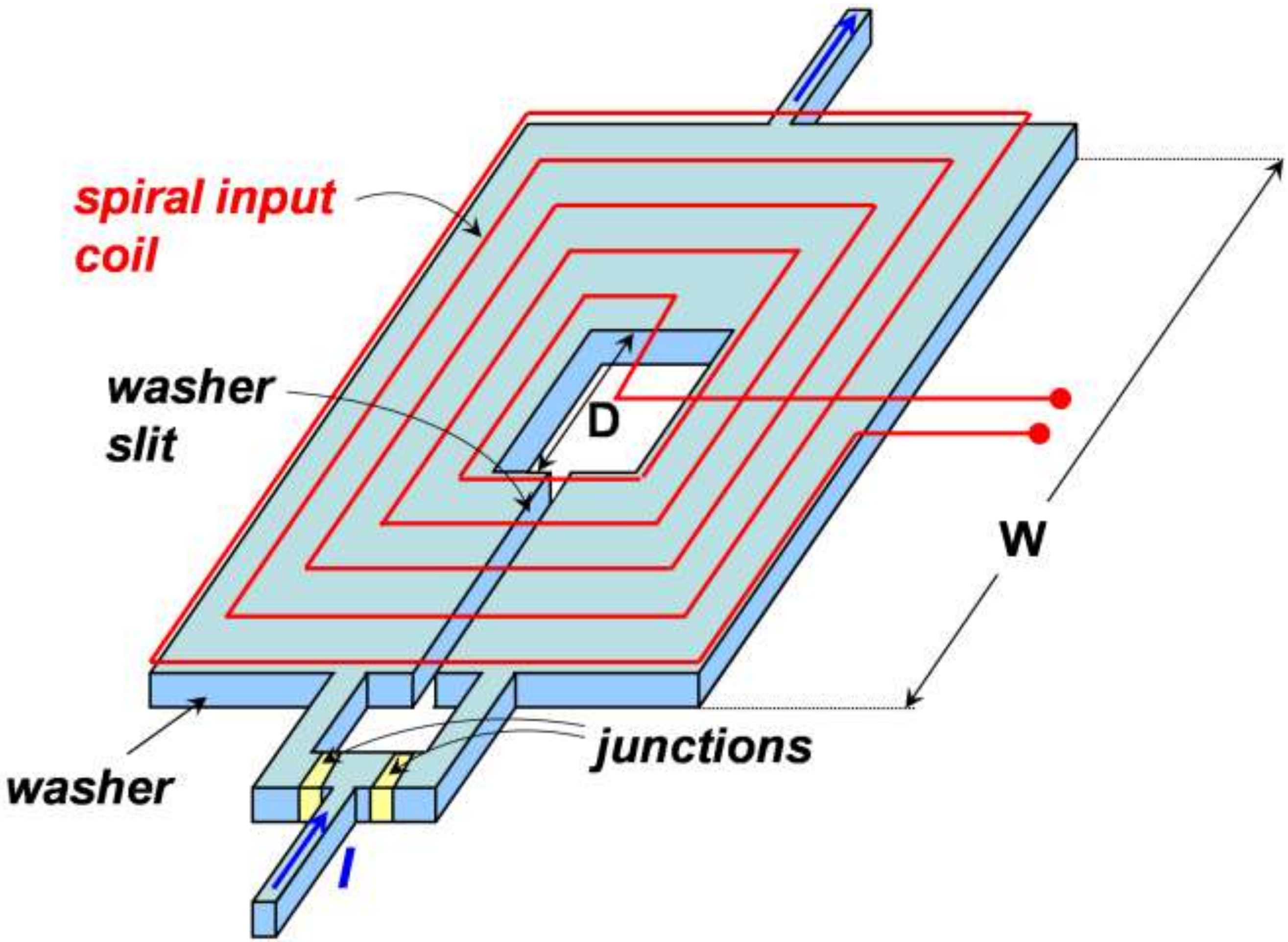

4.1.5 Readout schemes

Flux-locked loop operation

$\langle V\rangle(\Phi_{\mathrm{ext}})$ curve is nonlinear
→ Linearization by feedback circuit
→ Linear input – output relation

→ Apply oscillating flux with peak-to-peak amplitude $\frac{\Phi_0}{2}$
→ $f_{\mathrm{mod}} \approx 100\ \mathrm{kHz} - \mathrm{several\ MHz}$

Quasistatic flux $= n\Phi_0$
→ Rectified input
→ $2f_{\mathrm{mod}}$-component
→ Lock-in signal at f_{mod} vanishes

Quasistatic flux $= \left(n + \frac{1}{4}\right)\Phi_0$
→ Only f_{mod}-component exists
→ Maximum lock-in output signal

Detection of ac voltage
→ Low-noise preamplifier
→ Cooled transformer for
SQUID impedance matching
→ Example: $R_{\mathrm{d}} \rightarrow N^2 R_{\mathrm{d}}$

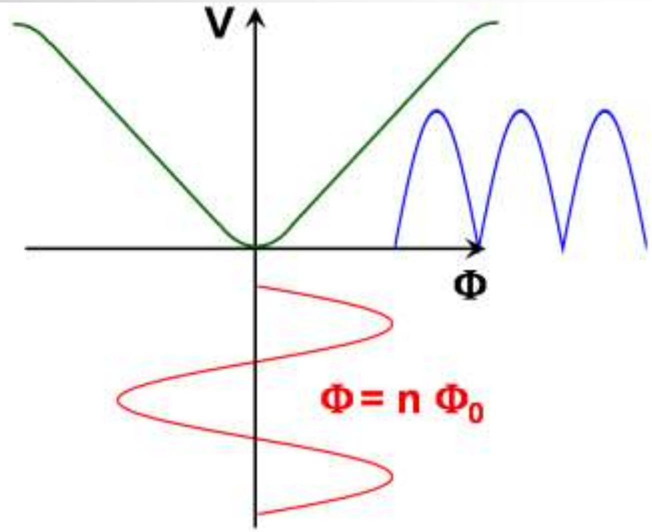

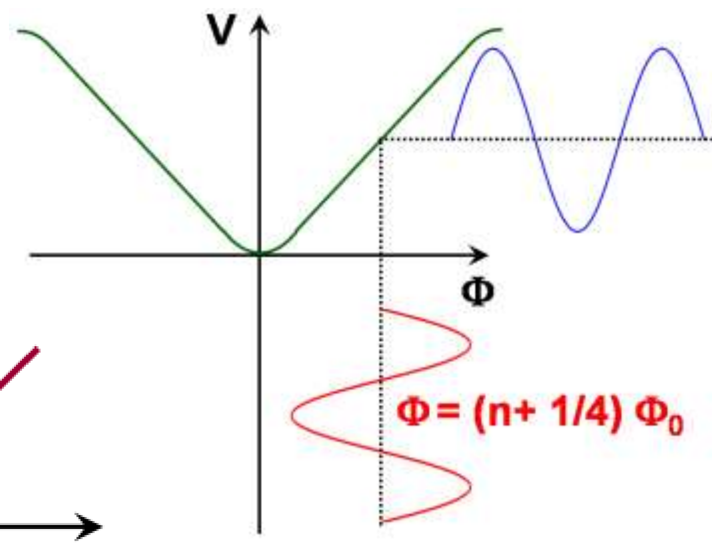

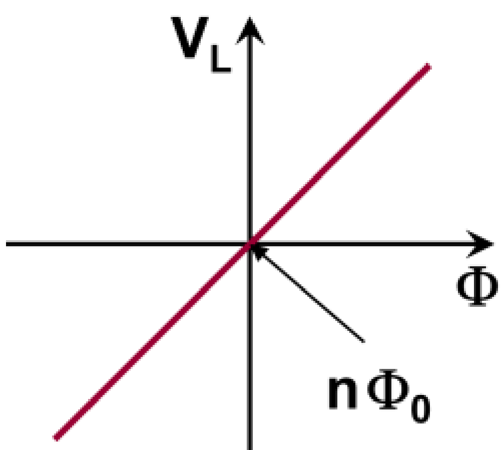

4.1.5 Readout schemes

Flux-locked loop operation

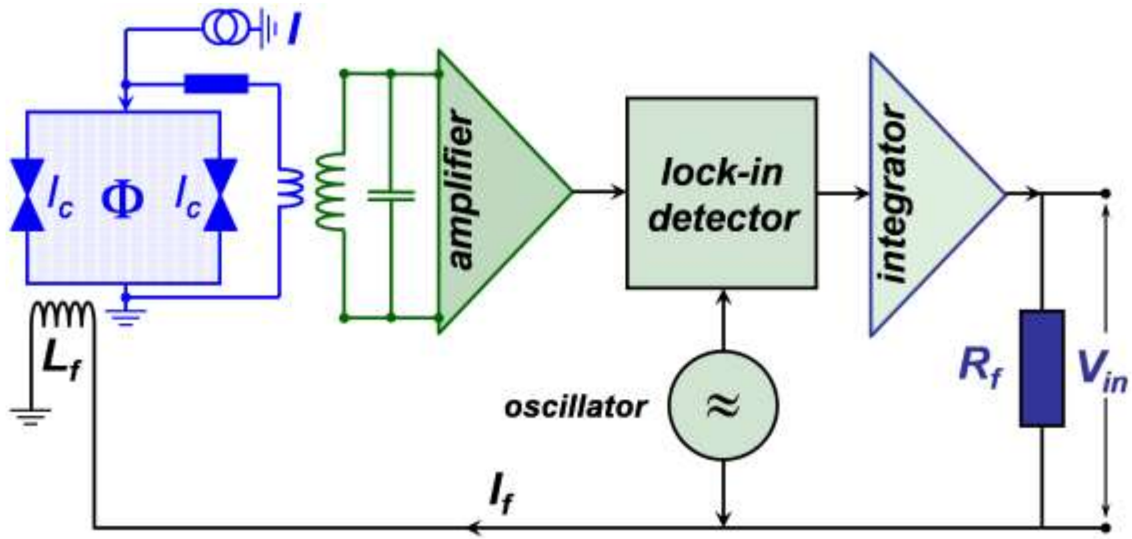

feedback coil with coupling constant k

Small flux change $\delta\Phi$ to SQUID → Positive output $\propto \delta\Phi$

→ Increase of integrator output voltage $\delta V_{\mathrm{in}} \propto \delta\Phi$
→ Increase of current through feedback coil
→ Feedback flux must compensate $\delta\Phi$ → $|\delta\Phi_{\mathrm{f}}| = |\delta\Phi|$
→ SQUID voltage (and integrator output) stay constant → Null detector

$$\delta I_{\mathrm{f}} = \frac{\delta V_{\mathrm{in}}}{R_{\mathrm{f}}},\ \delta\Phi_{\mathrm{f}} = k^2 L_{\mathrm{f}} \delta I_{\mathrm{f}} \quad \xrightarrow{|\delta\Phi_{\mathrm{f}}| = |\delta\Phi|} \quad \delta V_{\mathrm{in}} = \frac{R_{\mathrm{f}}}{k^2 L_{\mathrm{f}}} \delta\Phi$$

Specs of readout electronics

→ $f_{\mathrm{mod}} \approx 100\ \mathrm{kHz} - \mathrm{several\ MHz}$, bandwidth $\simeq 100\ \mathrm{kHz}$, dynamic range $\simeq 140\ \mathrm{dB}$
→ Slew rate (maximum compensation rate) up to $10^7\ \Phi_0/\mathrm{s}$

4.1.5 Readout schemes

Bias current reversal

→ Bias current is modulated → Double modulation technique
→ Suppress low-frequency noise of Josephson junctions
→ Asymmetric part of critical current fluctuations can be eliminated

Additional positive feedback

→ Part of the bias current used to obtain asymmetric $\langle V \rangle(\Phi_{\mathrm{ext}})$
→ Steeper slope → Larger $\frac{\partial V}{\partial \Phi}$
→ Direct read-out with room temperature electronics

Digital read-out schemes

→ Cryogenic digital feedback schemes → Compact, wideband
→ Digitized output signals for transmission to room temperature

Relaxation oscillation schemes

→ Hysteretic junctions
→ SQUID shunted by series LR-circuit
→ Frequency of relaxation oscillations depends on flux
→ Large SQUID output voltage

4.2 The rf SQUID

Superconducting loop with a single Josephson junction

→ Rf current is applied via a tank circuit inductively coupled to SQUID loop

→ Measure time-averaged tank circuit voltage

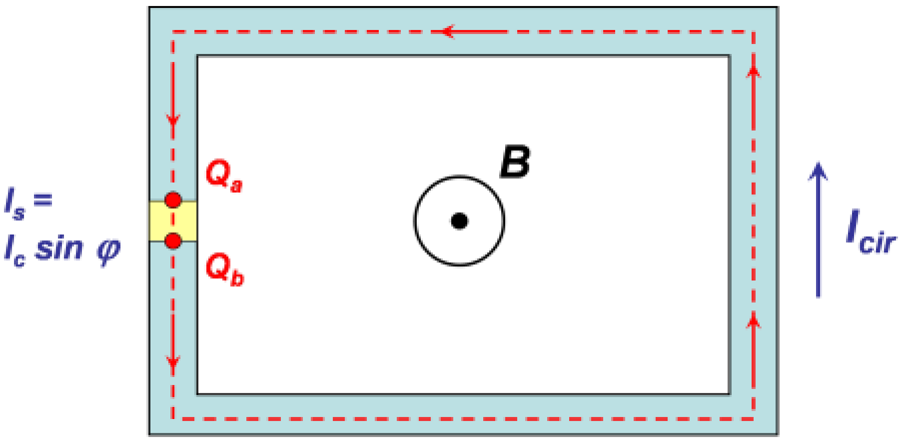

Advantage

→ Simpler fabrication, no dc-current to SQUID

Disadvantage

→ Energy resolution limited by readout electronics

Flux-phase relation (exercises)

→ $\varphi = -2\pi \frac{\Phi}{\Phi_0}$

4.2.1 The zero voltage state

Flux screening

$$\rightarrow \quad I_s = I_c \sin\left(-\frac{2\pi\Phi}{\Phi_0}\right) = -I_c \sin\frac{2\pi\Phi}{\Phi_0}$$

Supercurrent

$$\Phi = \Phi_{\text{ext}} + L I_{\text{cir}} = \Phi_{\text{ext}} - L I_c \sin\frac{2\pi\Phi}{\Phi_0}$$

Total flux

Screening parameter $\beta_{L,\text{rf}} \equiv 2\pi \frac{LI_\text{c}}{\Phi_0}$

$$\Rightarrow \frac{\Phi}{\Phi_0} = \frac{\Phi_{\text{ext}}}{\Phi_0} - \frac{\beta_{L,\text{rf}}}{2\pi} \sin\left(2\pi\frac{\Phi}{\Phi_0}\right)$$

$\beta_{L,\text{rf}} > 1$

→ Instable regions

→ Negative slope

→ Practically relevant

$\Phi_{\text{ext}} = \Phi_{\text{ext,c}}$

→ Junction critical current reached

→ Flux quantum enters SQUID ring

→ Hysteresis loop

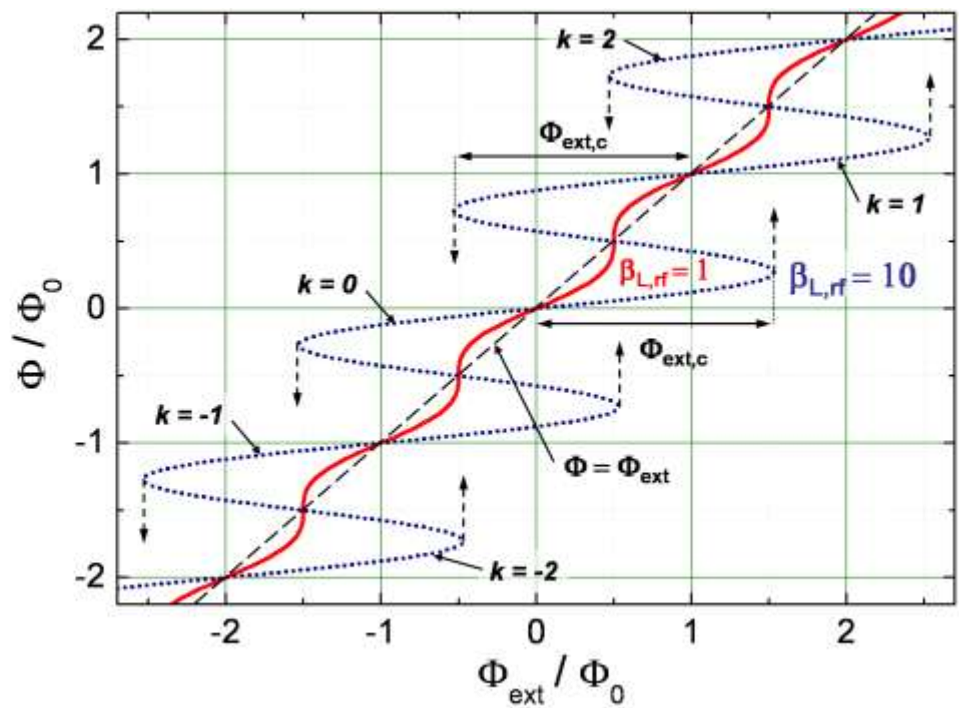

4.2.2 Operation and performance of rf SQUIDs

Operation of rf SQUIDs

→ SQUID loop inductively coupled to LC tank circuit

→ Quality factor $Q = \frac{R_\mathrm{T}}{\omega_\mathrm{rf} L_\mathrm{T}}$, where $\omega_\mathrm{rf}^2 = \frac{1}{L_\mathrm{T} C_\mathrm{T}}$

→ $I_\mathrm{T} = Q I_\mathrm{rf}$ → rf current in tank circuit

→ Mutual inductance $M = \alpha\sqrt{L_\mathrm{T} L}$

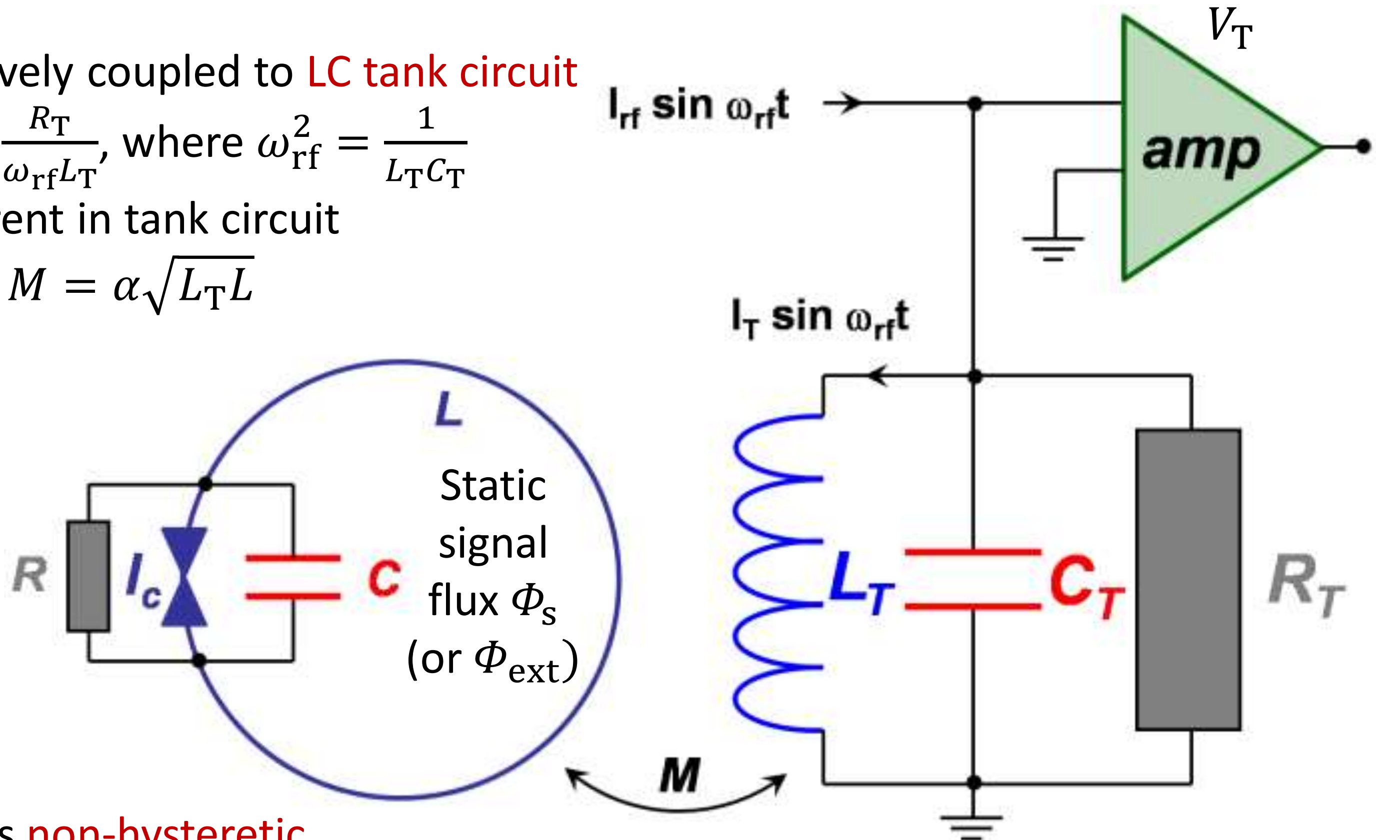

$\beta_{L,\mathrm{rf}} < 1$ → $\Phi(\Phi_\mathrm{ext})$ is non-hysteretic

→ Rf-SQUID behaves as nonlinear inductor

→ Modulation of the resonance frequency $\frac{1}{\sqrt{L_\mathrm{T,eff} C_\mathrm{T}}}$ (periodic with applied flux)

→ Operation close to ω_rf → Strong change in rf-voltage V_T → Flux-to-voltage transducer

4.2.2 Operation and performance of rf SQUIDs

$\beta_{L,\mathrm{rf}} > 1$

→ $\Phi(\Phi_{\mathrm{ext}})$ hysteretic

→ Applied flux through SQUID

$$\Phi_{\mathrm{ext}} = \Phi_{\mathrm{s}} + \Phi_{\mathrm{rf}} \sin \omega_{\mathrm{rf}} t$$
$$\Phi_{\mathrm{rf}} = M I_{\mathrm{T}} = M Q I_{\mathrm{rf}}$$

→ Linear increase of Φ_{rf}

→ Linear increase of V_{T} for $\Phi_{\mathrm{s}} + \Phi_{\mathrm{rf}} < \Phi_{\mathrm{ext,c}}$

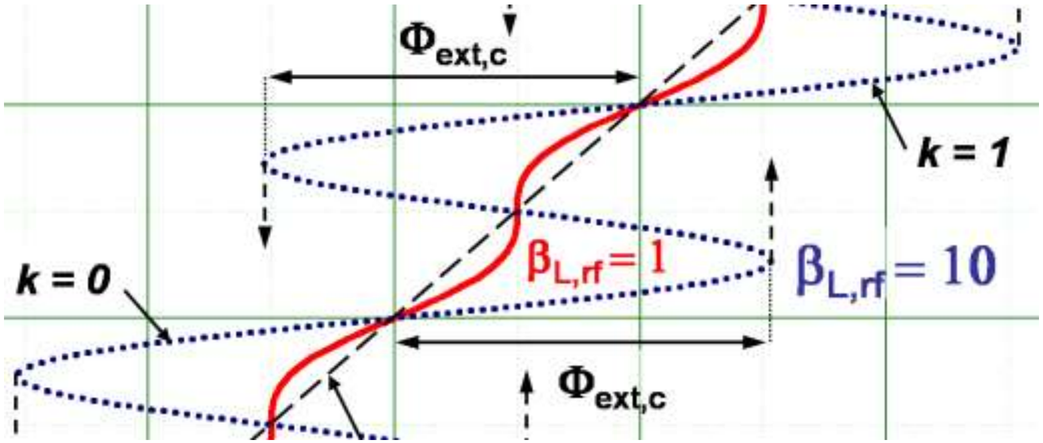

For $\Phi_{\mathrm{s}} + \Phi_{\mathrm{rf}} > \Phi_{\mathrm{ext,c}}$ → Hysteresis loop

→ Energy loss ∝ hysteresis loop area extracted from tank circuit

→ Damping of tank circuit

→ Damping is proportional to the area of a traced-out hysteresis loop

→ Also for $\beta_{L,\mathrm{rf}} > 1$ → Tank voltage is periodic in applied flux

4.2.2 Operation and performance of rf SQUIDs

Dependence of V_{T} on Φ_s and Φ_{rf}

Start at $\Phi_{\mathrm{s}} = n\Phi_0, n = 0$

→ Tank voltage V_T increases linearly with I_{rf} as long as $\Phi_{\mathrm{rf}} = MQI_{\mathrm{rf}} < \Phi_{\mathrm{ext,c}}$ (0 → A)

→ Critical rf-current $I_{\mathrm{rf,c}} \equiv \frac{\Phi_{\mathrm{ext,c}}}{MQ}$

$$V_{\mathrm{T}}^{(n=0)}(\Phi_{\mathrm{ext,c}}) = \omega_{\mathrm{rf}} L_{\mathrm{T}} I_{\mathrm{T,c}} = \omega_{\mathrm{rf}} L_{\mathrm{T}} \frac{\Phi_{\mathrm{ext,c}}}{M}$$

→ For $I_{\mathrm{rf}} > I_{\mathrm{rf,c}}$ → Jump to $k = \pm 1$ branch

→ Hysteresis loop, energy loss of tank circuit

→ Decrease of rf-current in tank circuit

→ No hysteresis loops until tank circuit recovers

→ Further increase of I_{rf} (A → B)

- → Transitions at higher rate
- → $I_{\mathrm{rf}} = I_{\mathrm{rf,r}}$ → One transition per rf cycle
- → Linear increase of $V_{\mathrm{T}}^{(n=0)}$ until jumps to $k = \pm 2$ branch become possible

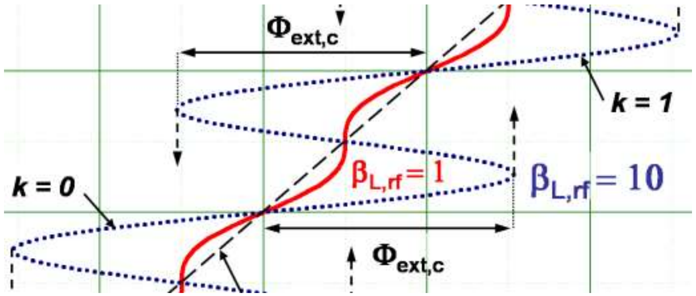

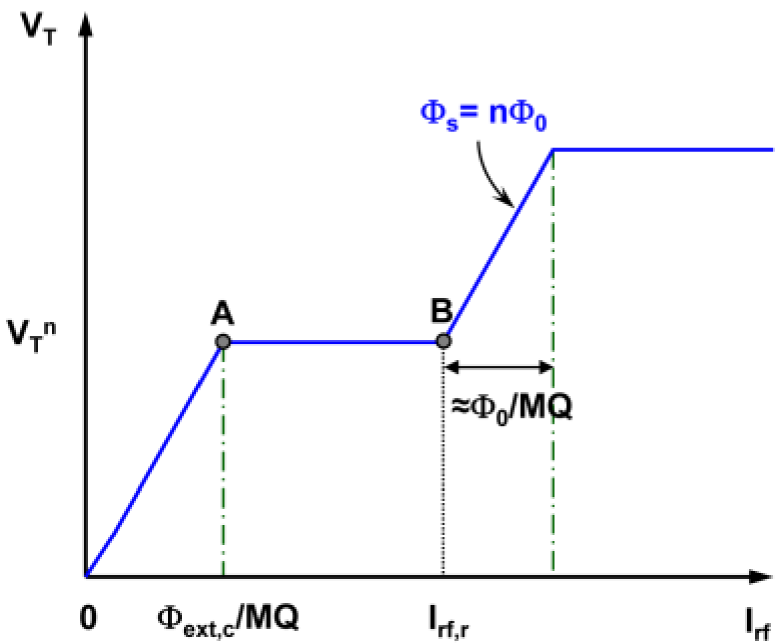

Dependence of V_{T} on Φ_s (signal) and Φ_{rf}

Start at $\Phi_{\mathrm{s}} = \left(n + \frac{1}{2}\right)\Phi_0,\ n = 0$

→ Transition to $k = \pm 1$ branch at $\pm\left(\Phi_{\mathrm{ext,c}} \mp \frac{\Phi_0}{2}\right)$

→ 1st horizontal branch at

$$V_{\mathrm{T}}^{(n=0.5)} = \omega_{\mathrm{rf}} L_{\mathrm{T}} \frac{\Phi_{\mathrm{ext,c}} - \Phi_0/2}{M}$$

Intermediate signal flux values

→ $V_T^{(n)}(I_{\mathrm{rf}})$ curves between those for $n = 0$ and $n = 0.5$

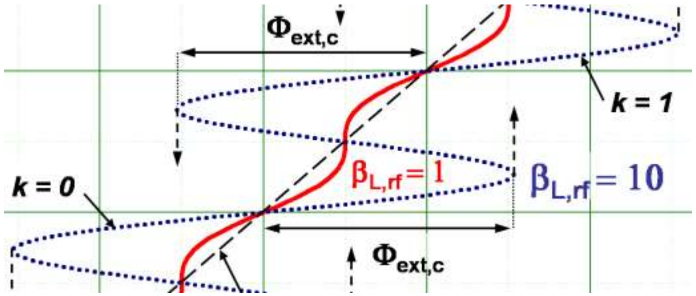

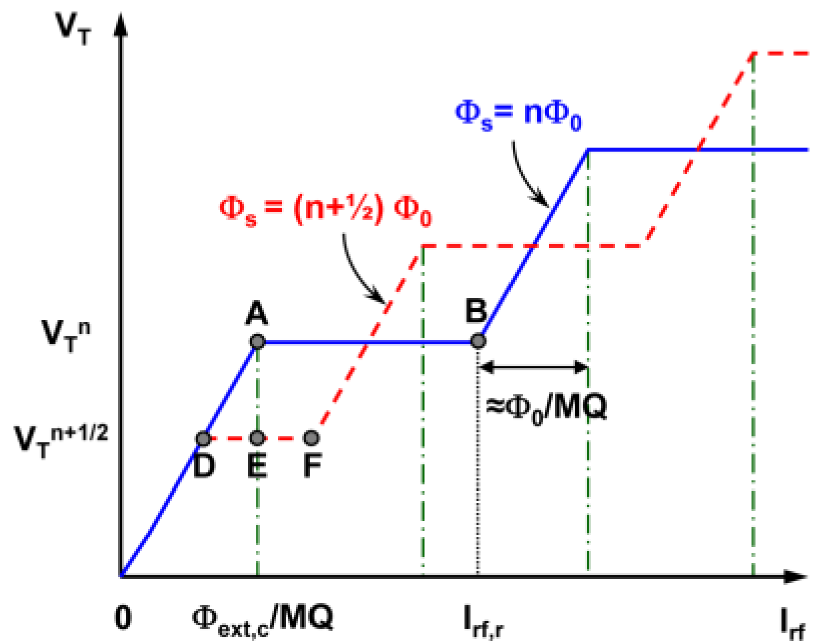

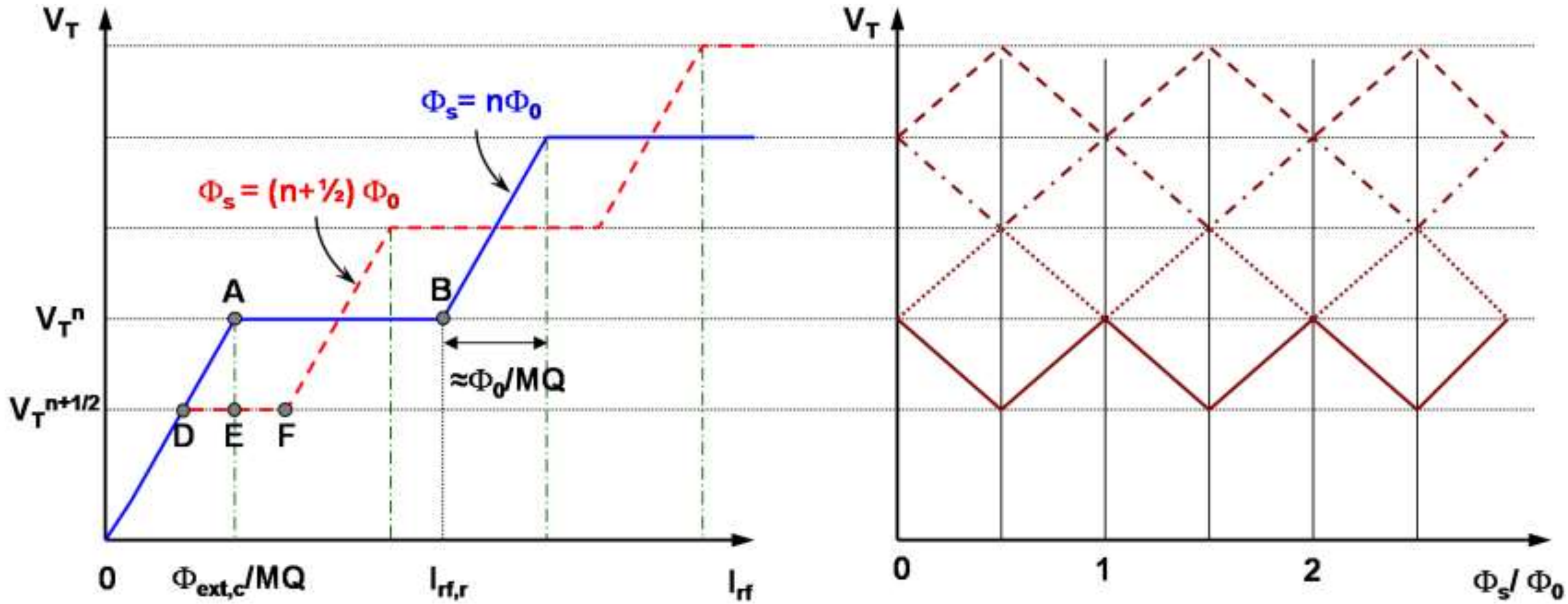

Change of V_T from $\Phi_\mathrm{s} = 0$ to $\Phi_\mathrm{s} = \frac{\Phi_0}{2} \rightarrow \frac{\omega_{rf} L_T \Phi_0}{2M}$

→ Flux-to-voltage transfer function near $\Phi_\mathrm{s} = \frac{\Phi_0}{4} \rightarrow H = \left(\frac{\partial V_\mathrm{T}}{\partial \Phi_\mathrm{s}}\right)_{I_\mathrm{rf}=const.} = \frac{\omega_\mathrm{rf} L_\mathrm{T}}{M}$

→ Lower bound for $M \propto \alpha \rightarrow \forall \Phi_\mathrm{s}$, there must be an I_rf that intersects the first step of $V_T(I_\mathrm{rf})$ (point F has to be to the right of E)

$$\rightarrow H \approx \frac{\omega_\mathrm{rf} L_\mathrm{T}}{\alpha\sqrt{L_T L}} = \omega_{rf}\sqrt{Q\,\frac{L_\mathrm{T}}{L}}$$

→ Practical operation with flux-locked loop scheme → Stay on one step for all Φ_s

Noise in rf SQUIDs

Mechanism

→ Switching $k = 0 \rightarrow k = 1$ → Stochastic fluctuations (thermal activation)

→ Noise in step voltage V_T → Flux noise $S_\Phi \approx \frac{(LI_c)^2}{\omega_{rf}} \left(\frac{2\pi k_B T}{I_c \Phi_0}\right)^{4/3}$ or $\eta^2 \equiv \frac{S_\Phi \omega_{rf}}{\pi \Phi_0^2}$

→ Noise causes finite slope of horizontal branches

→ Extrinsic noise sources (preamplifier, lines) → T_{amp}^{eff}

→ Energy resolution $\epsilon \approx \left(\frac{\pi \eta^2 \Phi_0^2}{2L} + 2\pi \eta k_B T_{amp}^{eff}\right) \frac{1}{\omega_{rf}}$

→ High frequencies (few GHz), cryogenic amplifiers: $\epsilon \simeq 3 \times 10^{-32}$ J/Hz

Comparison

→ Rf SQUID $\epsilon \approx \frac{k_B T}{\omega_{rf}}$ $(\omega_{rf} \simeq \text{few GHz})$

→ Dc SQUID $\epsilon \approx \frac{k_B T}{\omega_c}$ $\left(\omega_c = \frac{2\pi I_c R_N}{\Phi_0} \simeq 100 \text{ GHz}\right)$

→ Better energy resolution of dc-SQUID because $\omega_c \gg \omega_{rf}$

4.2.3 Practical rf-SQUIDs

Low-T_c rf SQUIDs

→ Early versions were toroidal configuration machined from Nb
→ Operated at 10 MHz with $\epsilon \simeq 5 \times 10^{-29}$ J/Hz
→ Today thin film technology → $\epsilon \simeq 10^{-32}$ J/Hz

High-T_c rf-SQUIDs

→ Operating at 77 K (liquid nitrogen)
→ Washer-type rf-SQUIDs incorporated in a $\lambda/2$ microstrip resonator

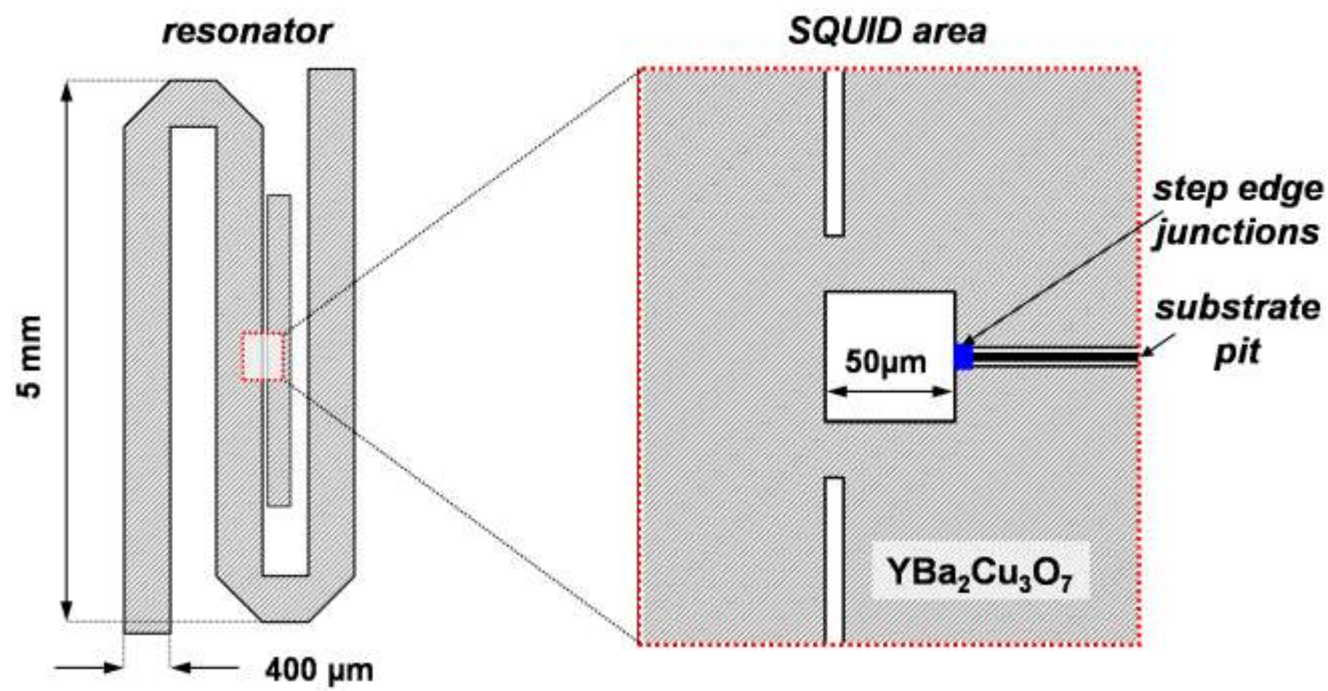

4.3 Additional topic: Other SQUID configurations

Motivation

→ Dc and rf SQUID are the most obvious configurations
→ Over the years, many other configurations have been developed
→ Specific advantages and disadvantages
→ Examples discussed here: DROS, SQUIF, cartwheel SQUID

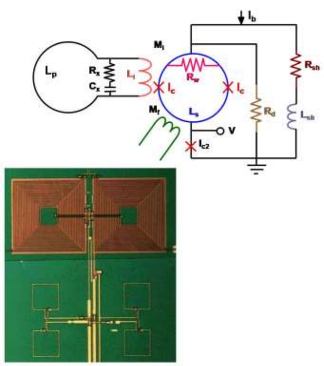

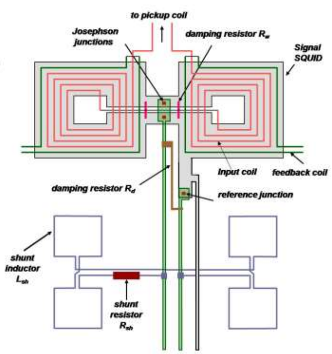

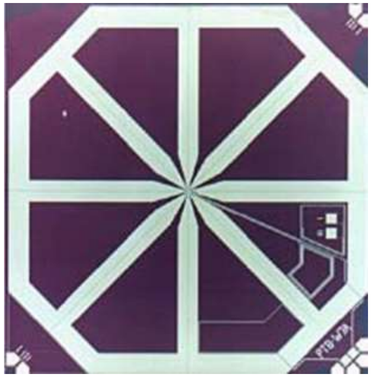

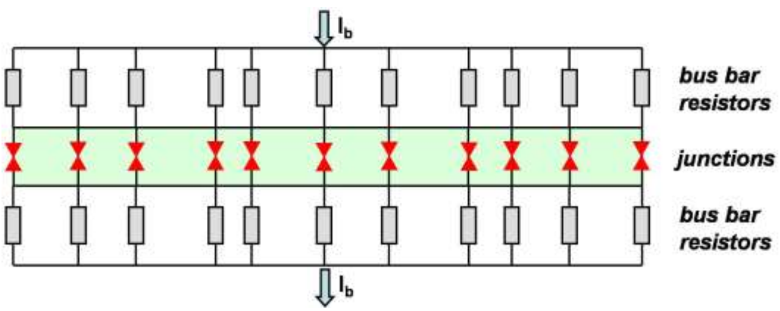

4.3.1 Additional topic:
The DROS (Double Relaxation Oscillation SQUID)

Hysteretic dc-SQUID ($\beta_C > 1$) + hysteretic reference junction in series + LR shunt

→ System performs relaxation oscillations

→ DROS functions as comparator of the two critical currents

→ Voltage output behaves like square wave

→ Large flux-to-voltage transfer coefficients up to $3\ \mathrm{mV}/\Phi_0$

→ Direct read-out by RT amplifier

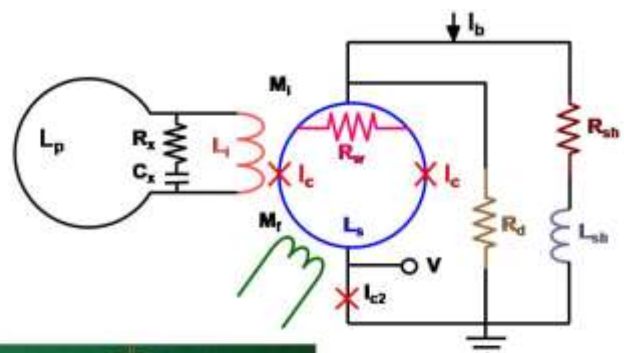

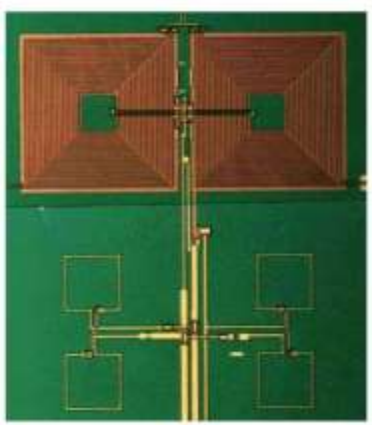

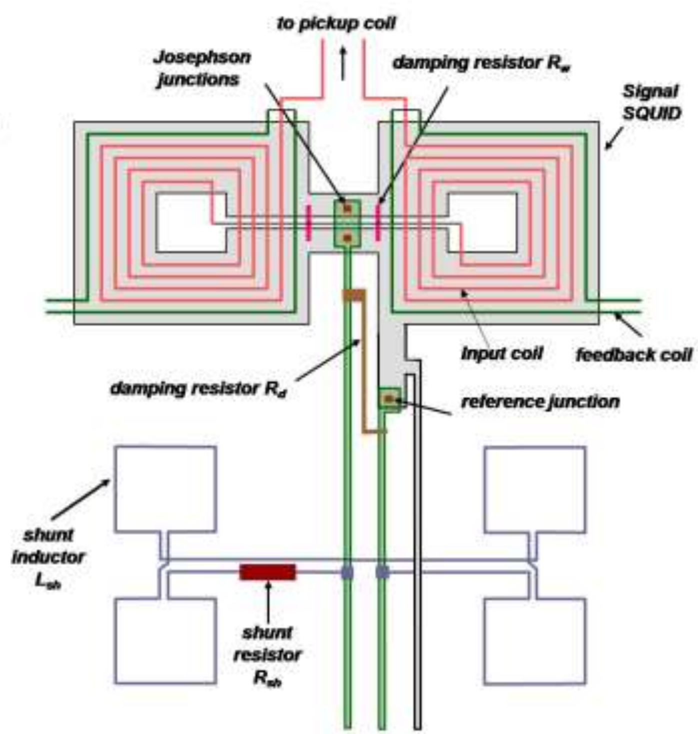

4.3.2 Additional topic: The SQIF

Motivation

→ $\beta_L \ll 1$ → Dc-SQUID analogous to double slit configuration
→ Steeper $I_s^{\mathrm{m}}(\Phi_{\mathrm{ext}})$ inspired by optical grid analog → N junctions in parallel
→ Experimental problem → Uniformity of junctions and loops

Irregular parallel array of JJ

→ Superconducting Quantum Interference Filter (SQUIF)
→ $I_s^{\mathrm{m}}(\Phi_{\mathrm{ext}})$ and $\langle V\rangle(\Phi_{\mathrm{ext}})$ show a sharp peak at zero flux
→ Large $\frac{\partial V}{\partial \Phi_{\mathrm{ext}}}$

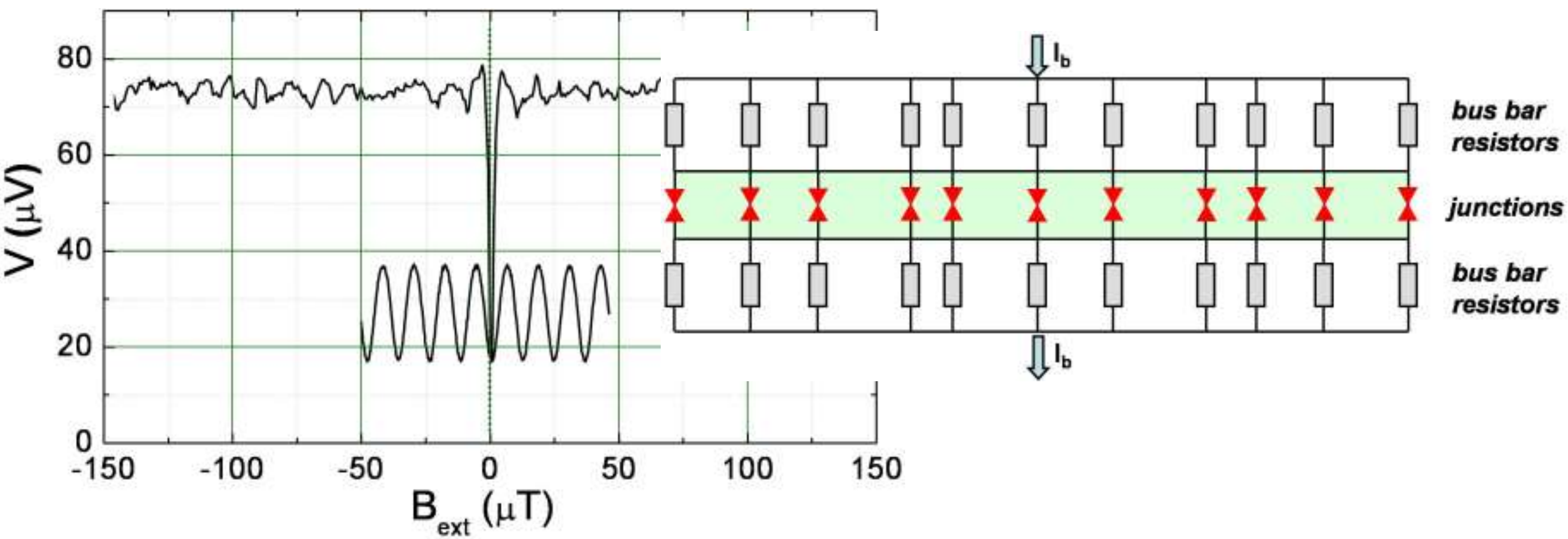

4.3.3 Additional topic: Cartwheel SQUID

SQUID loop → Several loops in parallel → reducing total SQUID loop inductance

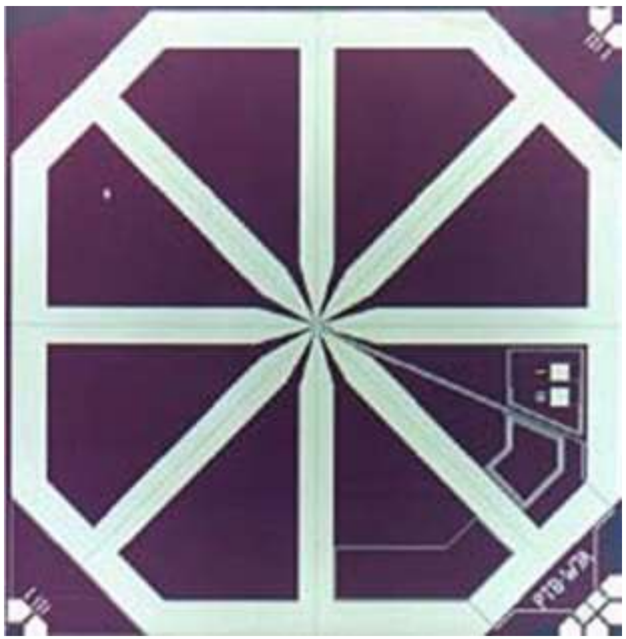

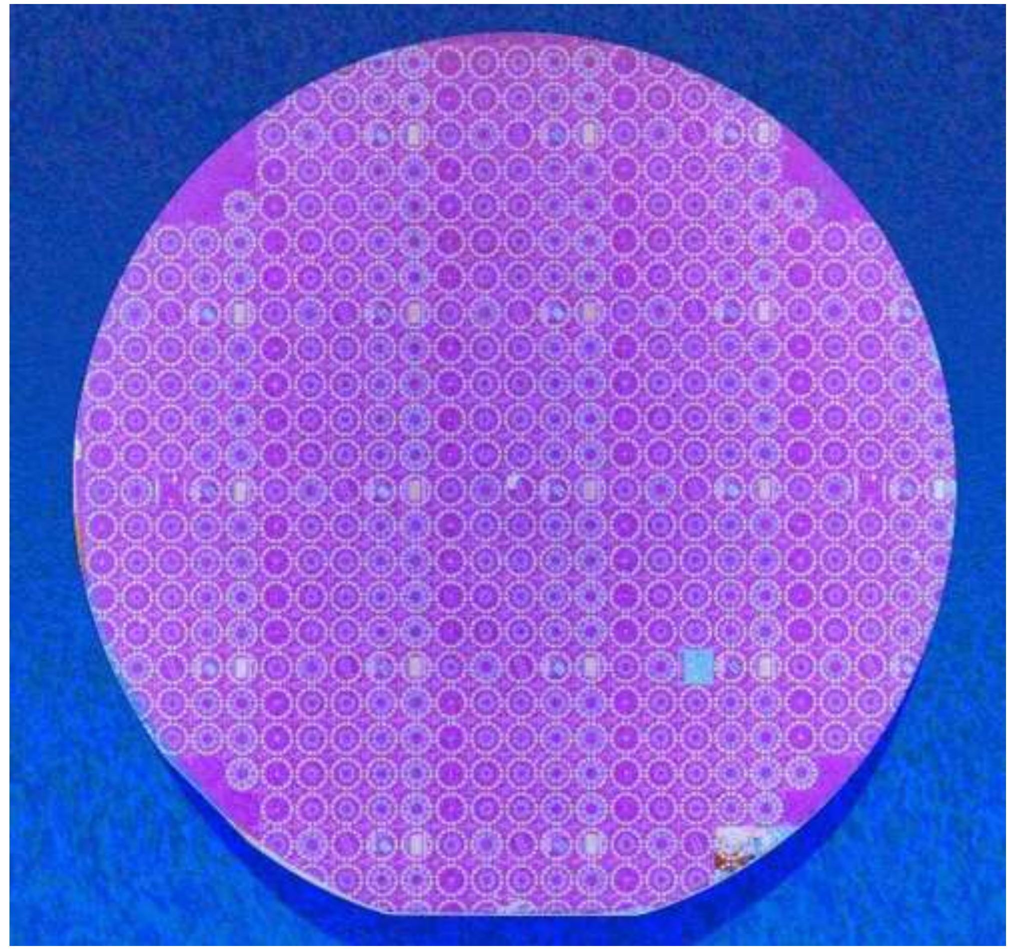

4.4 Instruments Based on SQUIDs

SQUIDs sense any signal that can be converted to flux

SQUID based instrument → Antenna determines quantity to be measured

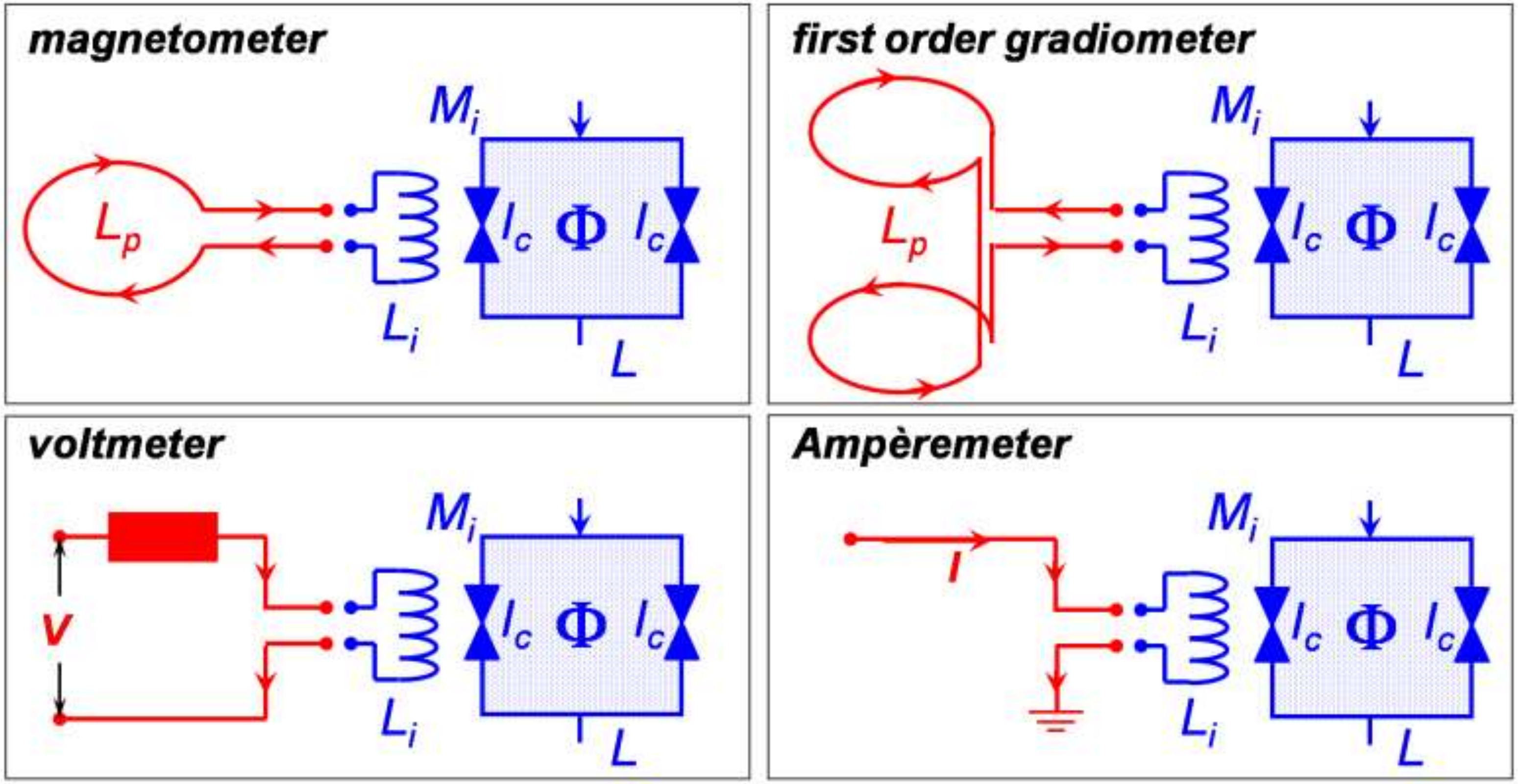

Input circuit influences signal and noise properties of SQUID

Reduction of SQUID inductance to

$$L' = L - \frac{M^2}{L_i + L_p} = L\left(1 - \frac{\alpha^2 L_i}{L_i + L_p}\right)$$

α^2 = coupling coefficient

Mutual inductance: $M_i = \alpha\sqrt{L_i L}$

Flux change in input coil: $\delta\Phi^{\mathrm{p}} = N_{\mathrm{p}} A_{\mathrm{p}} \delta B_{\mathrm{ext}}$

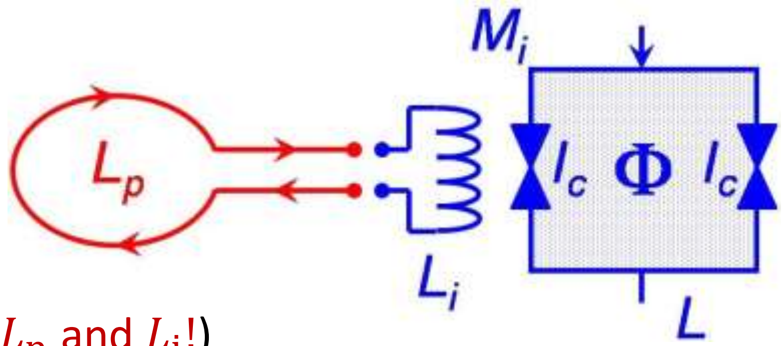

→ Shielding current I_{sh} in pickup and input coil
→ Flux coupled to SQUID

Flux quantization (superconducting contact between L_{p} and L_{i}!)

$$\delta\Phi^p + (L_i + L_p) I_{\mathrm{sh}} = N_p A_p \delta B_{\mathrm{ext}} + (L_i + L_p) I_{\mathrm{sh}} = 0$$

Flux coupled to SQUID operating in flux locked loop

$$\delta\Phi = M_i |I_{\mathrm{sh}}| = M_i \frac{\delta\Phi^p}{L_i + L_p} = \frac{\alpha\sqrt{L_i L}}{L_i + L_p} \delta\Phi^p = \frac{\alpha\sqrt{L_i L}}{L_i + L_p} N_p A_p \delta B_{\mathrm{ext}}$$

Minimum detectable $\delta\Phi^{\mathrm{p}}$ → Compare $\delta\Phi$ and equivalent SQUID flux noise

Spectral flux noise density referred to pick-up loop:

$$S_\Phi^p = \frac{(L_i + L_p)^2}{M_i^2} S_\Phi = \frac{(L_i + L_p)^2}{\alpha^2 L_i L} S_\Phi$$

Equivalent noise energy referred to pick-up loop

$$\epsilon^p = \frac{S_\Phi^p}{2L_p} = \frac{(L_i + L_p)^2}{L_i L_p} \frac{S_\Phi}{2\alpha^2 L} = \frac{(L_i + L_p)^2}{L_i L_p} \frac{\epsilon}{\alpha^2}$$

Minimum for $L_{\mathrm{i}} = L_{\mathrm{p}}$

$$\epsilon^p(f) = \frac{4\epsilon(f)}{\alpha^2}$$

Matching of L_{i} and L_{p} → Maximum fraction $\frac{\alpha^2}{4}$ of the energy is transferred

4.4.1 Magnetometers

Thin film magnetometers

@ 4.2 K: wire wound L_p & planar multi-turn thin film input coil

Reminder: Superconducting contact between L_p and L_i!

HTS magnetometers

No flexible wires (prototypes exist already) → Thin film flux transformers

→ Directly coupled SQUID

→ Flip-chip arrangement of single layer flux transformer and SQUID

→ Flip-chip arrangement of multilayer flux transformer and SQUID

Multi-loop magnetometers

N loops in parallel → Reduction of total inductance & large effective area

Typically trilayer structures

Example → 8 loops, diameter 7.2 mm → Sensitivity $\simeq 1.5\,\frac{\mathrm{fT}}{\sqrt{\mathrm{Hz}}}$

4.4.1 Magnetometers

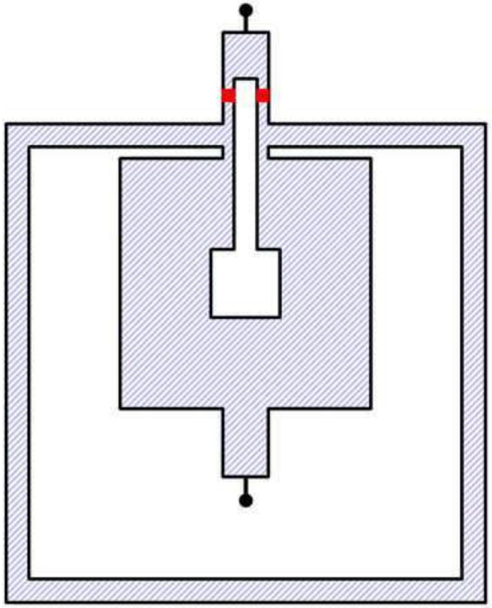

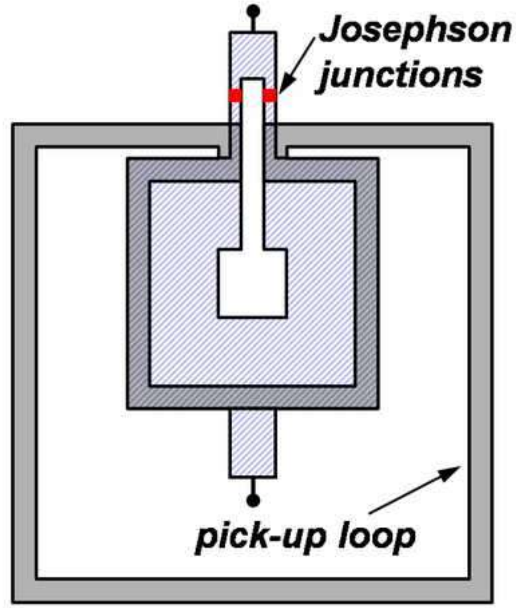

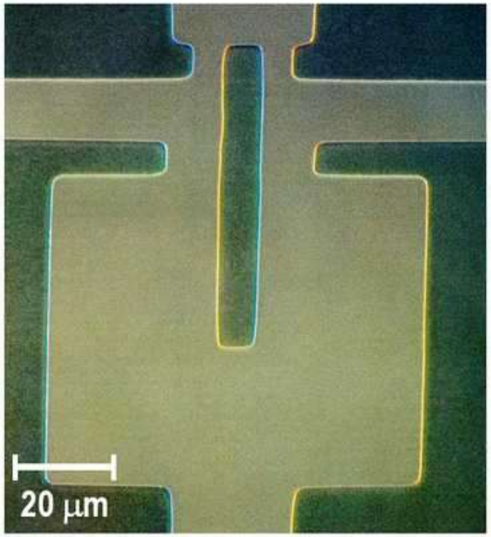

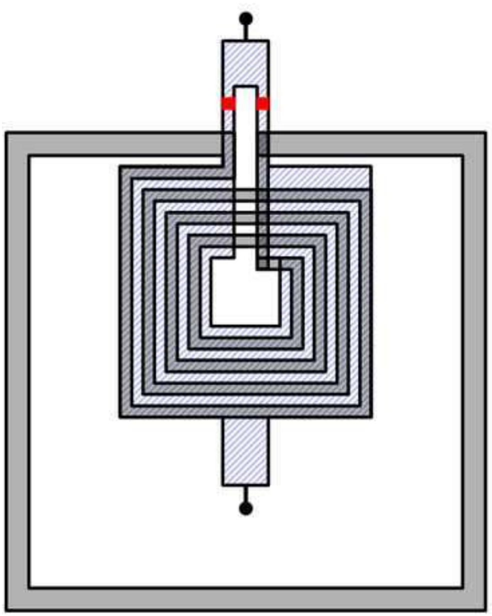

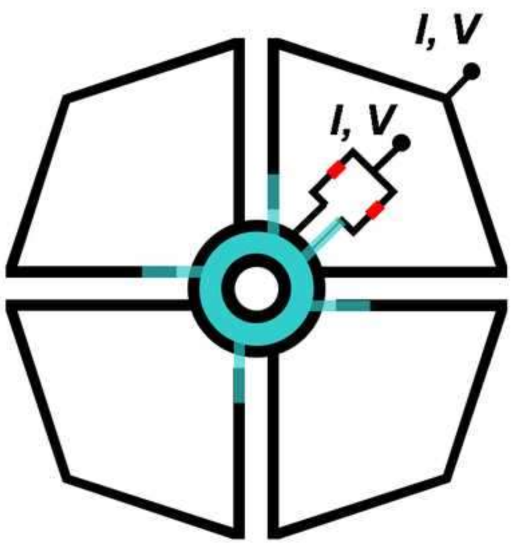

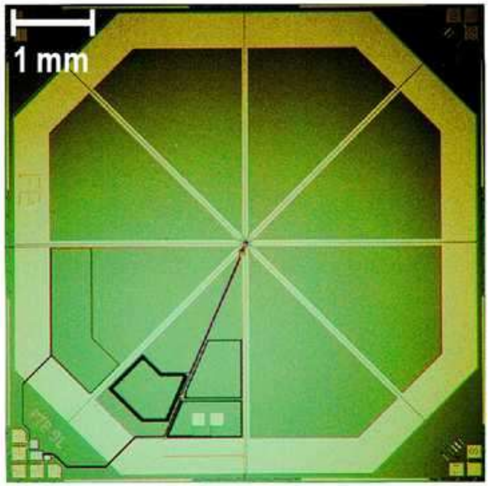

4.4.1 Magnetometers

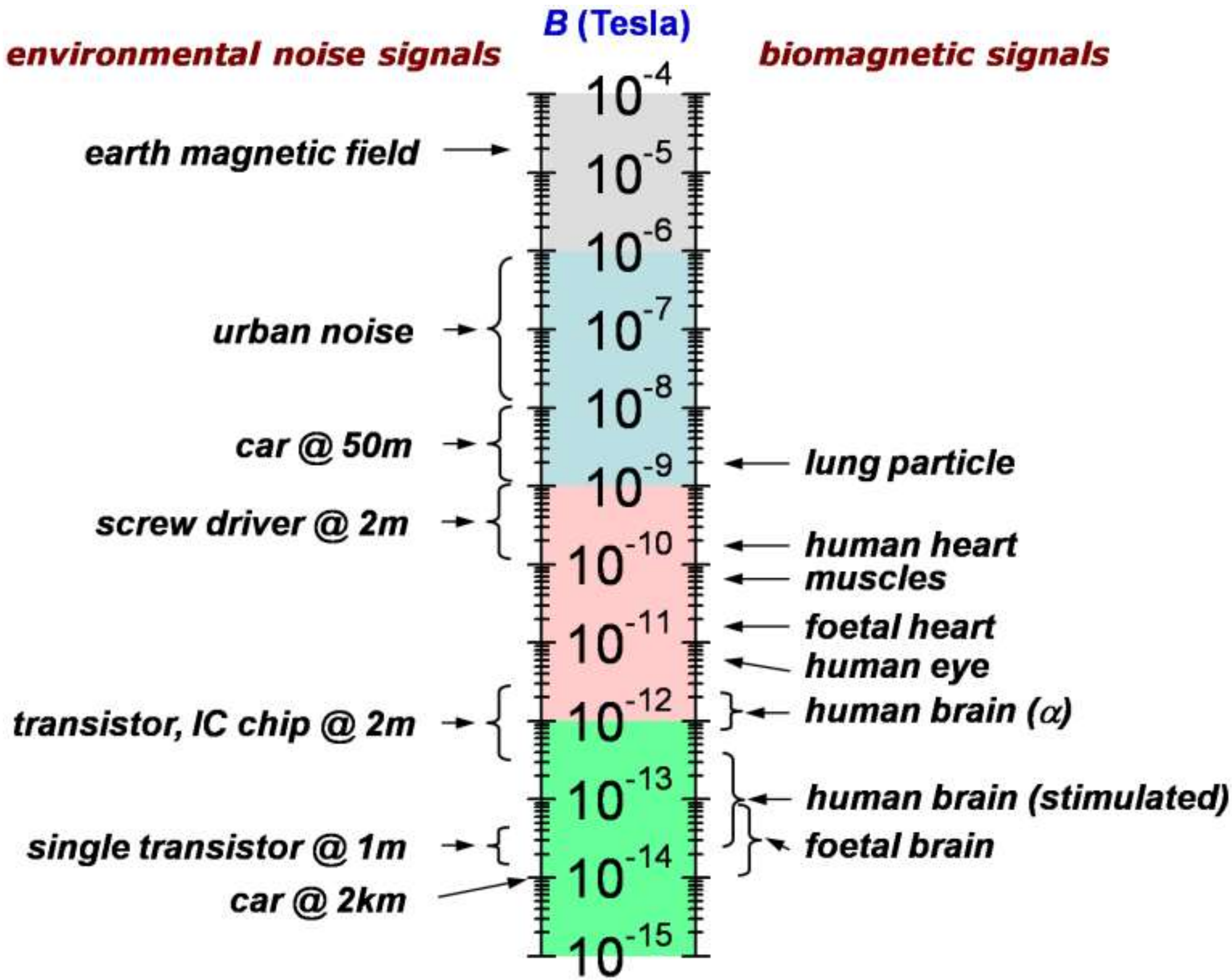

4.4.2 Gradiometers

For high-sensitivity measurements (e.g., biomagnetism)
→ Reduce perturbing environmental magnetic fields
→ Non-magnetic materials
→ High permeability shields (μ-metal or cryoperm)
→ Magnetically shielded rooms
→ Further reduction via gradiometers!

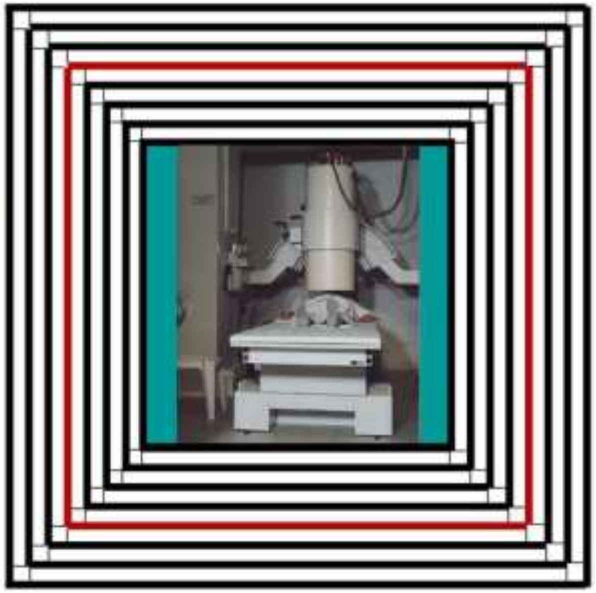

WMI qubit cryostat:
- 3 μ-metal cylindric pots (top is open) at room temperature
- 1 cryoperm pot at $4\ \mathrm{K}$
- Shielding factor: $\simeq 2 \times 10^3$ @ a few Hz
- Now further improved by superconducting Al or Pb pot at $50\ \mathrm{mK}$

PTB Berlin:
- 7 μ-metal shields
- 1 Al layer
- Active field reduction
- Shielding factor: 2×10^6 @ 0.01 Hz 2×10^8 @ 5 Hz

4.4.2 Gradiometers

axial gradiometer **planar gradiometer**

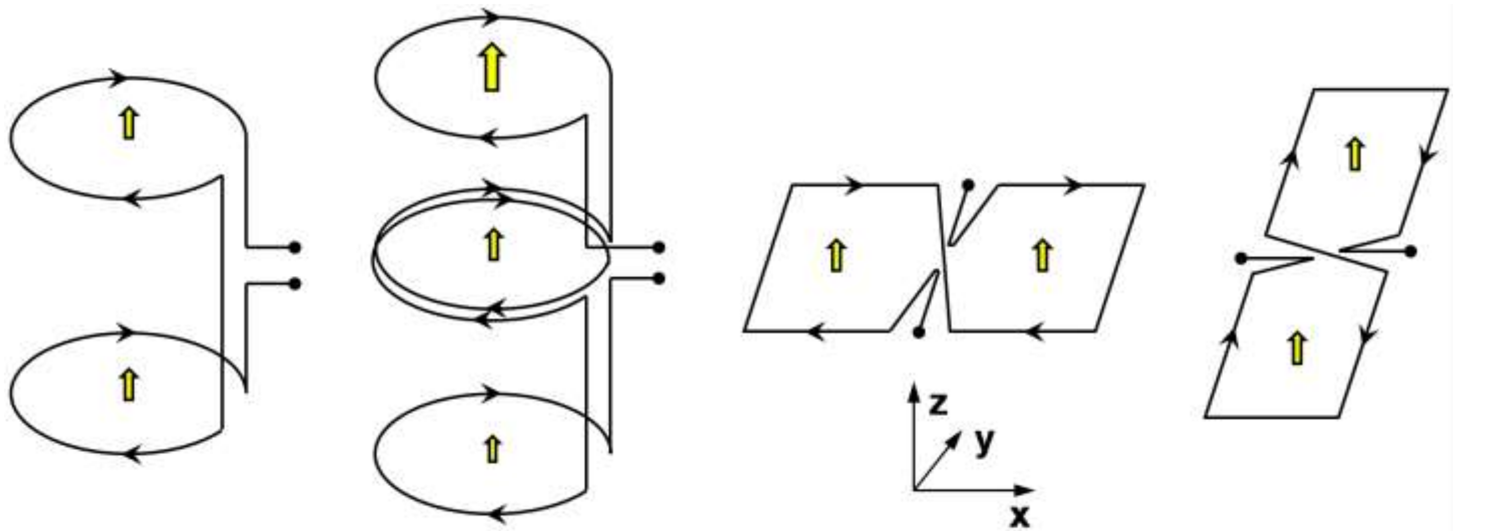

1st order 2nd order 1st order, dB_z/dx 1st order, dB_z/dy

n^{th}-order gradiometers

→ Suppression of uniform remote signals
→ Sensitive to field gradients

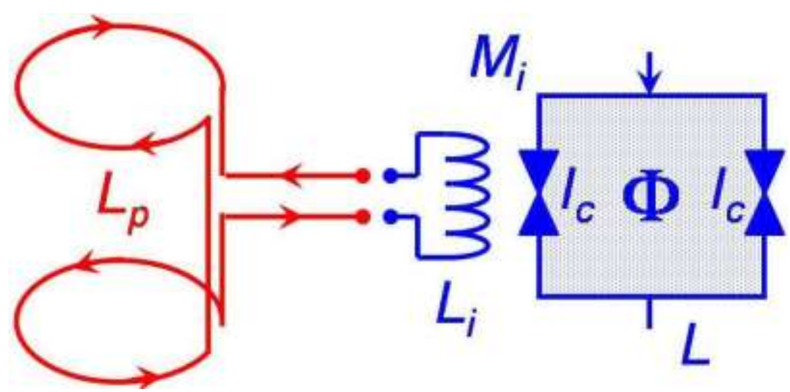

4.4.3 Susceptometers

Measurement of magnetic properties of materials

→ $\chi = \frac{M}{H}$ is response of magnetization to an external field
→ 1st or 2nd order gradiometer & sample in static B field
(gradiometer removes effect of static field)
→ Sample in one of the pick-up loops

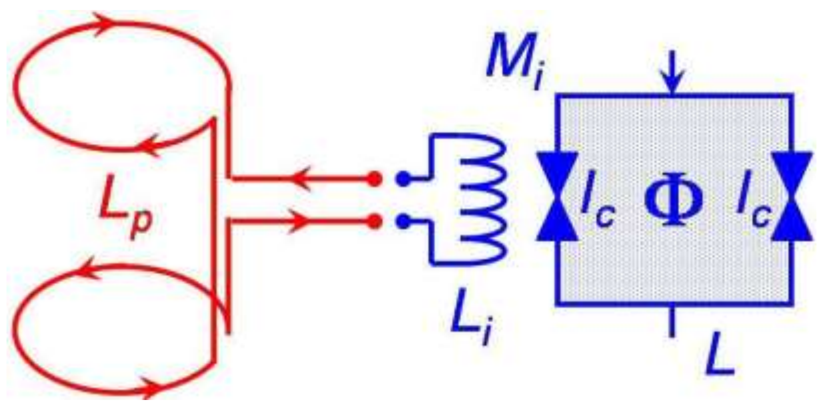

Non-magnetic sample → No output signal
Sample with susceptibility χ → Additional flux detected by SQUID

Commercial systems
→ 2nd order gradiometer
→ Sample axially moving
→ Resolution of 10^{-8} emu at $1.8 - 400$ K up to 7 T

Miniature susceptometer

→ $\chi_\mathrm{m} \equiv \frac{\partial M}{\partial H}, \mu_\mathrm{r} = 1 + \chi_\mathrm{m}$
→ 1st order gradiometer
→ Sample in one loop + global static field
  → Measure only response of the sample
→ For very small samples
→ SQUID loop
  → Two pick-up loops on SC ground plane
  → Minimize inductance
  → Sample in one loop
→ Sensitivity
Magnetization of
≃3000 electron spins

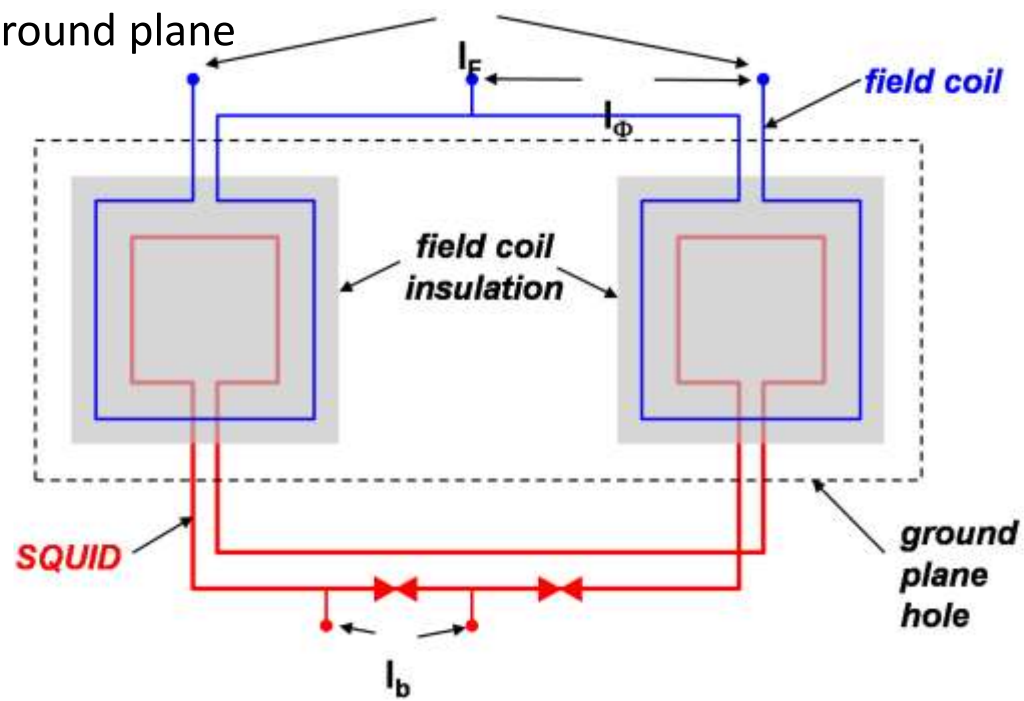

4.4.4 Voltmeters

Voltage transformed into current via input resistor
→ Feedback of SQUID output to input resistor
→ Flux locked loop (null-balancing of voltage)

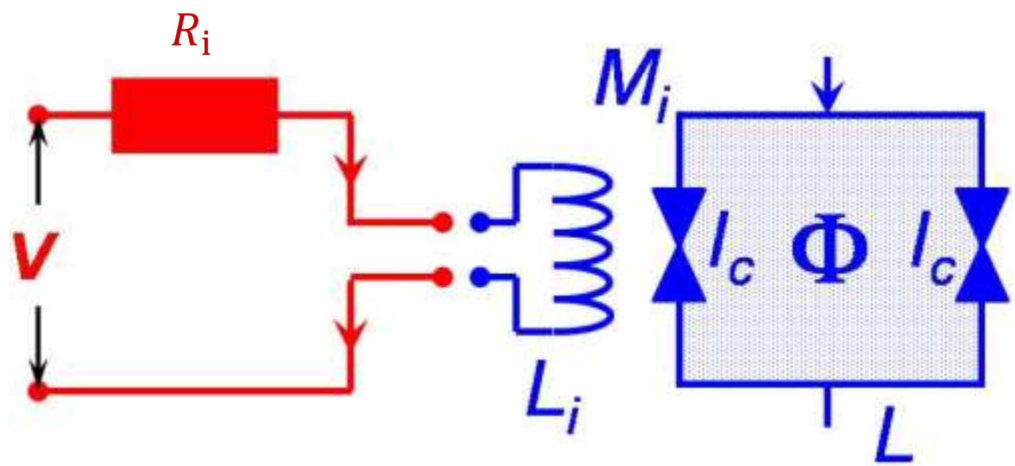

Resolution
→ $\simeq 10^{-12}\ \mathrm{V}/\sqrt{\mathrm{Hz}}$ for $R_\mathrm{i} = 0.01\ \Omega$
→ $\simeq 10^{-10}\ \mathrm{V}/\sqrt{\mathrm{Hz}}$ for $R_\mathrm{i} = 100\ \Omega$
→ Superior for low impedance samples

Applications:
→ Transport and noise measurments
→ Thermoelectric properties of metallic/superconducting samples

4.4.5 Radiofrequency amplifiers

Tuned amplifier

→ Input circuit: R_i , C_i, and L_i

→ For frequencies up to $100\ \mathrm{MHz}$

→ Noise temperature close to the quantum limit $\mathrm{T}_\mathrm{N}^\mathrm{QL} \approx \frac{\hbar\omega}{k_\mathrm{B} \ln 2}$

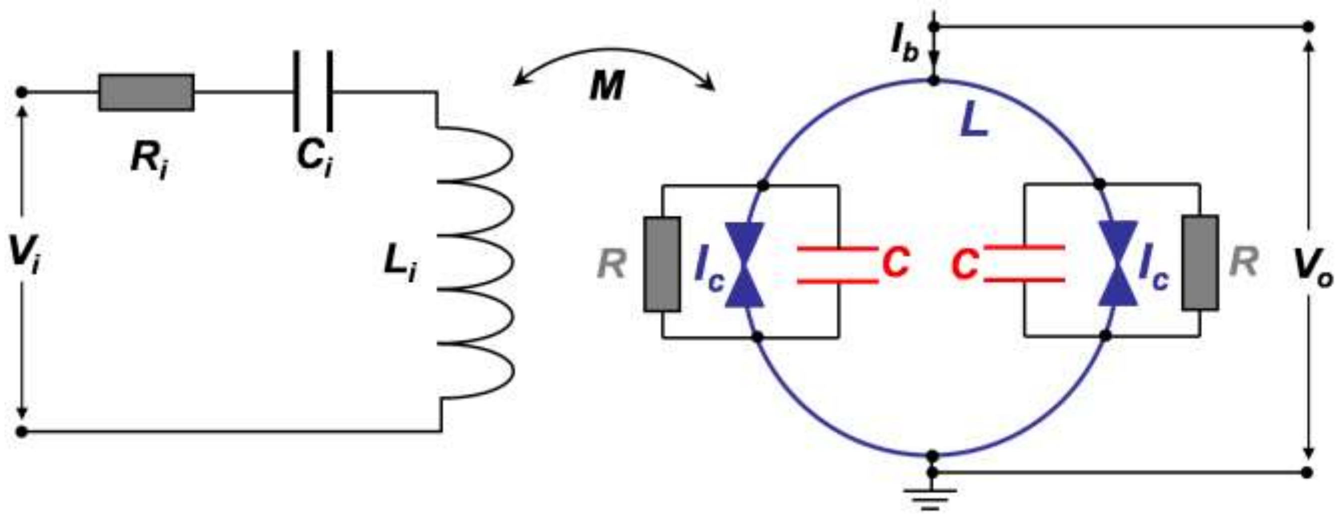

Motivation of the quantum limit for amplifiers

→ Bosonic input field mode $\hat{b}$ with commutation relation $\left[\hat{b}, \hat{b}^\dagger\right] = 1$

→ Linear amplification by factor $G \gg 1$ → Output mode $\hat{c} \equiv G\hat{b}$

→ $\left[\hat{c}, \hat{c}^\dagger\right] = G^2 \neq 1$, but must also be bosonic

→ Solution → Phase-insensitive amplifier must add noise!

4.5 Applications of SQUIDs

Detection of small signals is practically relevant in modern science and technology!

→ Biomagnetism
→ Nondestructive evaluation
→ Archeology
→ SQUID microscopy
→ Gravity wave detectors

4.5.1 Biomagnetism

Biomagnetic method

→ Non-invasive detection of magnetic signals from human body

Biomagnetic imaging

→ Field map of heart / brain activity
→ Source location via simple volume conductor models
→ MEG (magnetoencephalography) → Brain
→ MCG (magnetocardiography) → Heart

Extremely small fields
→ Brain $\simeq 100$ fT
Single neuron $\simeq 0.1$ fT
Heart $\simeq 100$ pT
→ Highly sensitive SQUID magnetometers
→ Low 1/f noise

Spatial and temporal magnetic field distribution
→ Scan single SQUID
→ SQUID sensor array (multichannel systems)

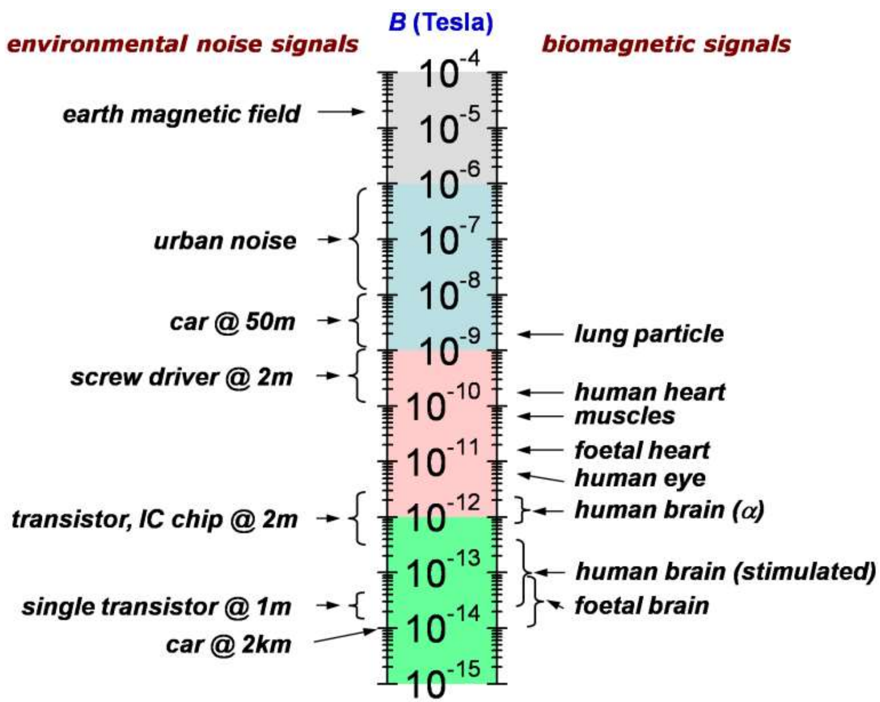

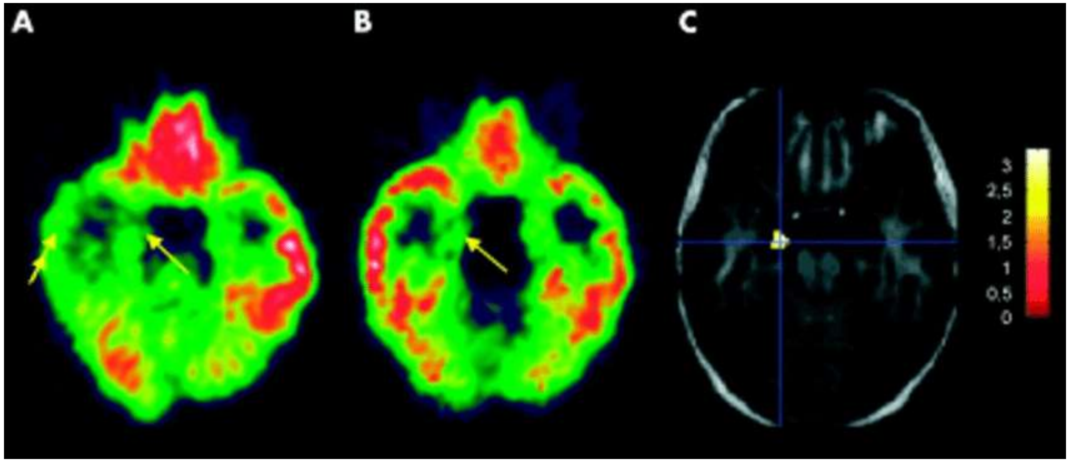

Signal reconstruction

→ Current distribution cannot be calculated from measured field distribution

→ Inverse problem has no unique solution

→ Model assumptions based on elementary current dipoles (short localized conductor segments & volume backflow)

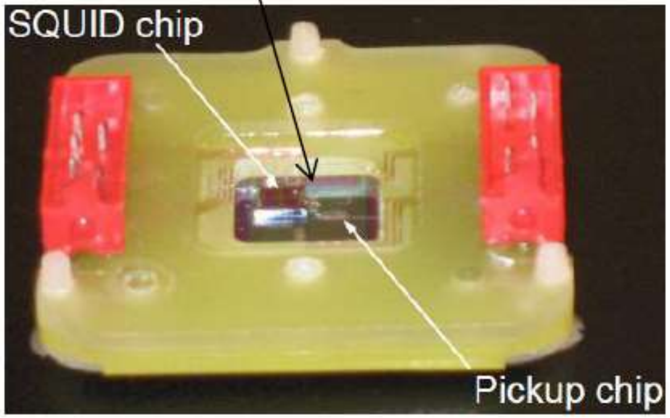

4.5.2 Nondestructive evaluation (NDE)

→ Non-invasive identification of structural or material defects
→ (Sub-) surface cracks in aircrafts
→ Reinforcing rods in concrete strutures
→ Short distance between inner cold and outer warm wall (spatial resolution)
→ HTS SQUIDs (@ 77 K) advantageous

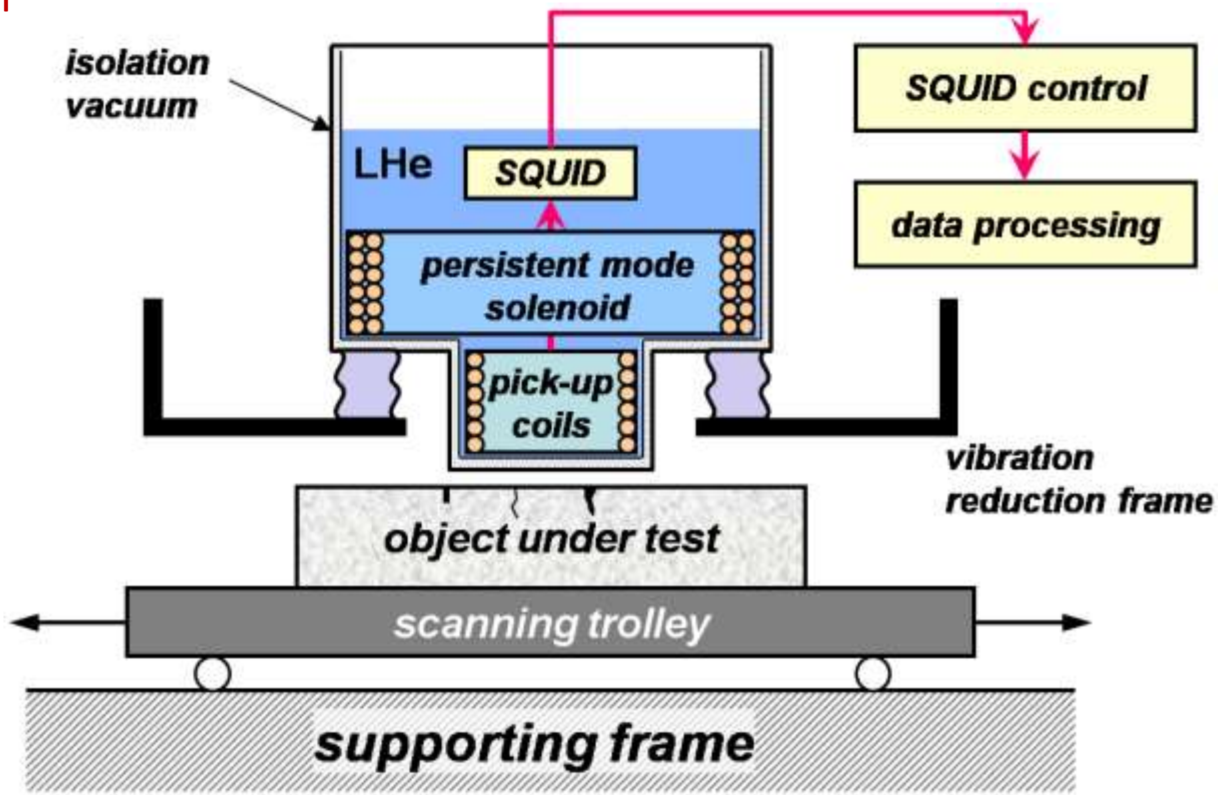

Eddy-current techniques

→ Alternating field
→ Eddy currents disturbed by material defects

4.5.2 Nondestructive evaluation (NDE)

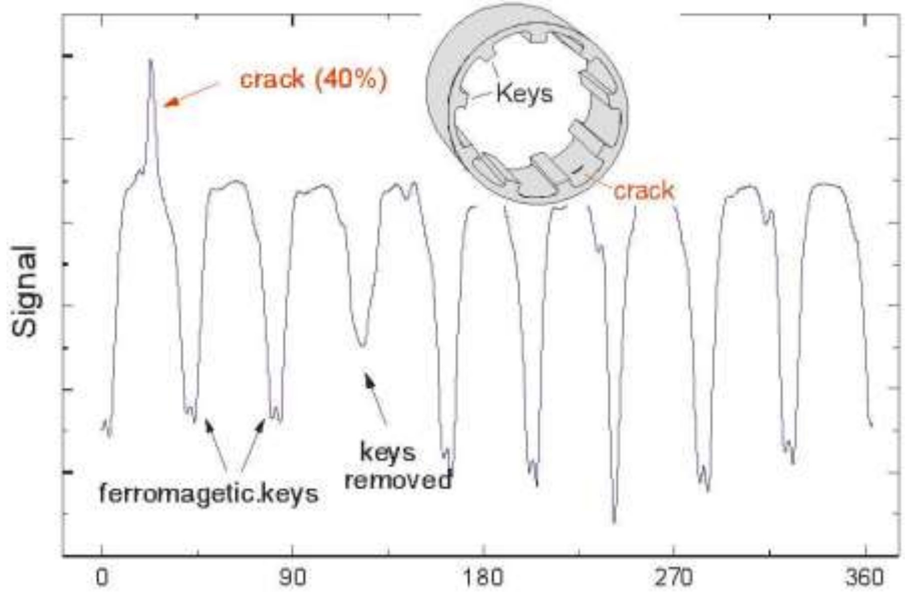

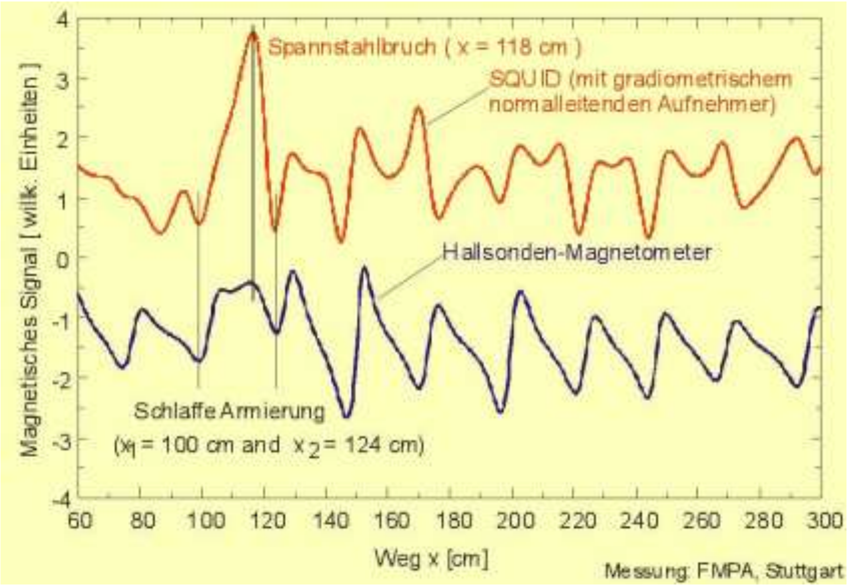

4.5.3 SQUID microscopy

Image magnetic field distribution

→ High sensitivity, modest spatial resolution
→ Initially low-T_c dc SQUIDs → now high-T_c SQUIDs @ 77 K
→ Frequency: dc up to 1 GHz

Spatial resolution
→ Cold samples $\simeq$ 5 μm (with soft magnetic focusing tip $\simeq$ 0.1 μm)
→ Room temperature samples $\simeq$ 30 – 50 μm

Applications
→ Diagnostics of SC devices
→ Properties of ultra-thin magnetic films
→ Analysis of semiconducting devices

SQUID-sample separation
→ 75 μm Sapphire window $\simeq$ 150 μm
→ 3 μm Si_xN_y window $\simeq$ 15 μm

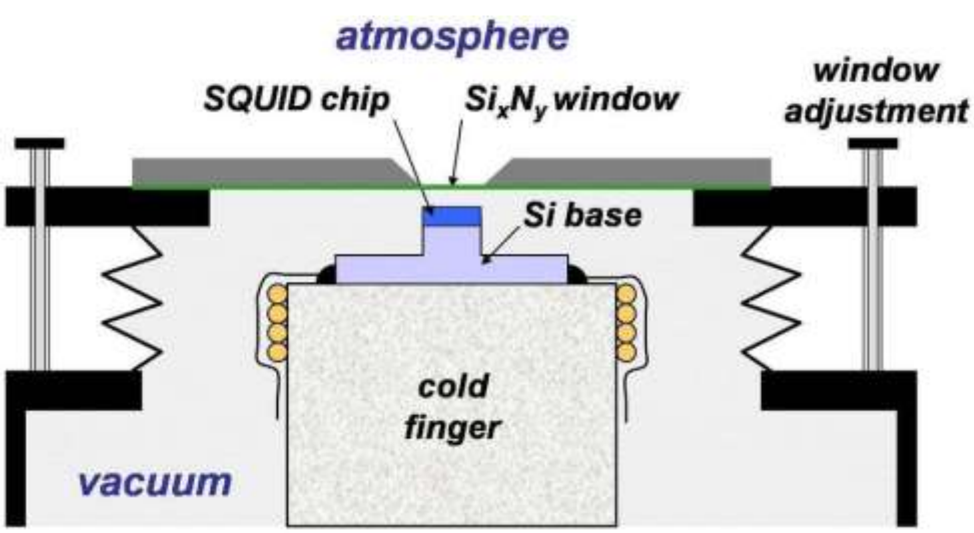

→ Scanning nano-SQUIDs
single-spin resolution

4.5.3 SQUID Microscopy

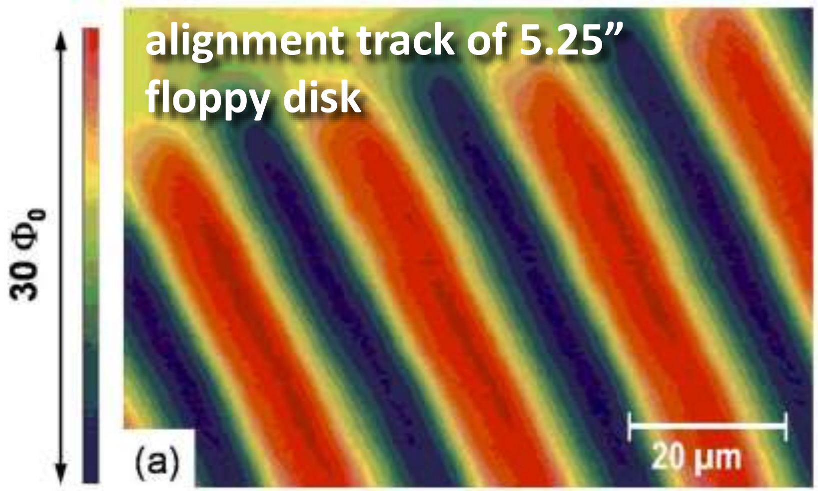

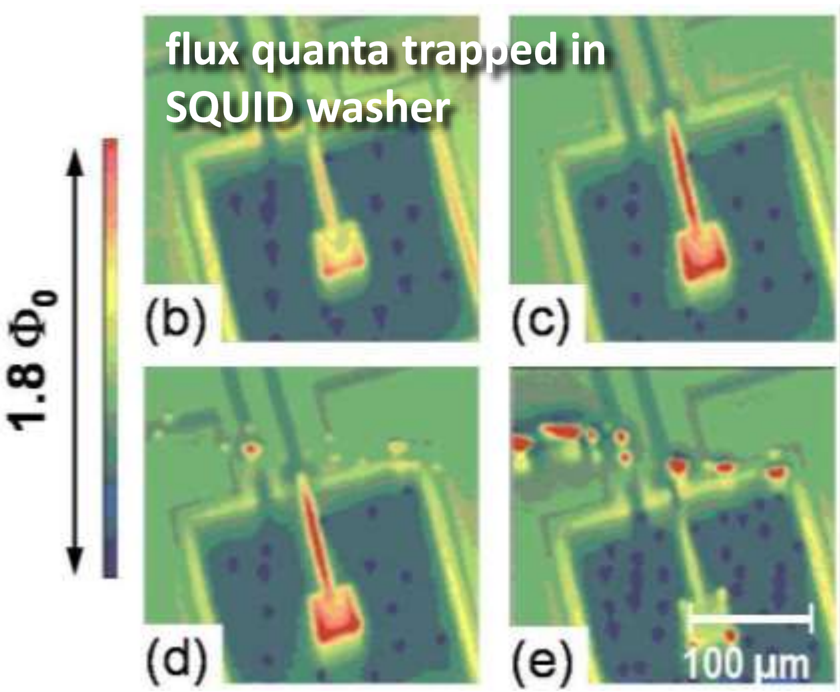

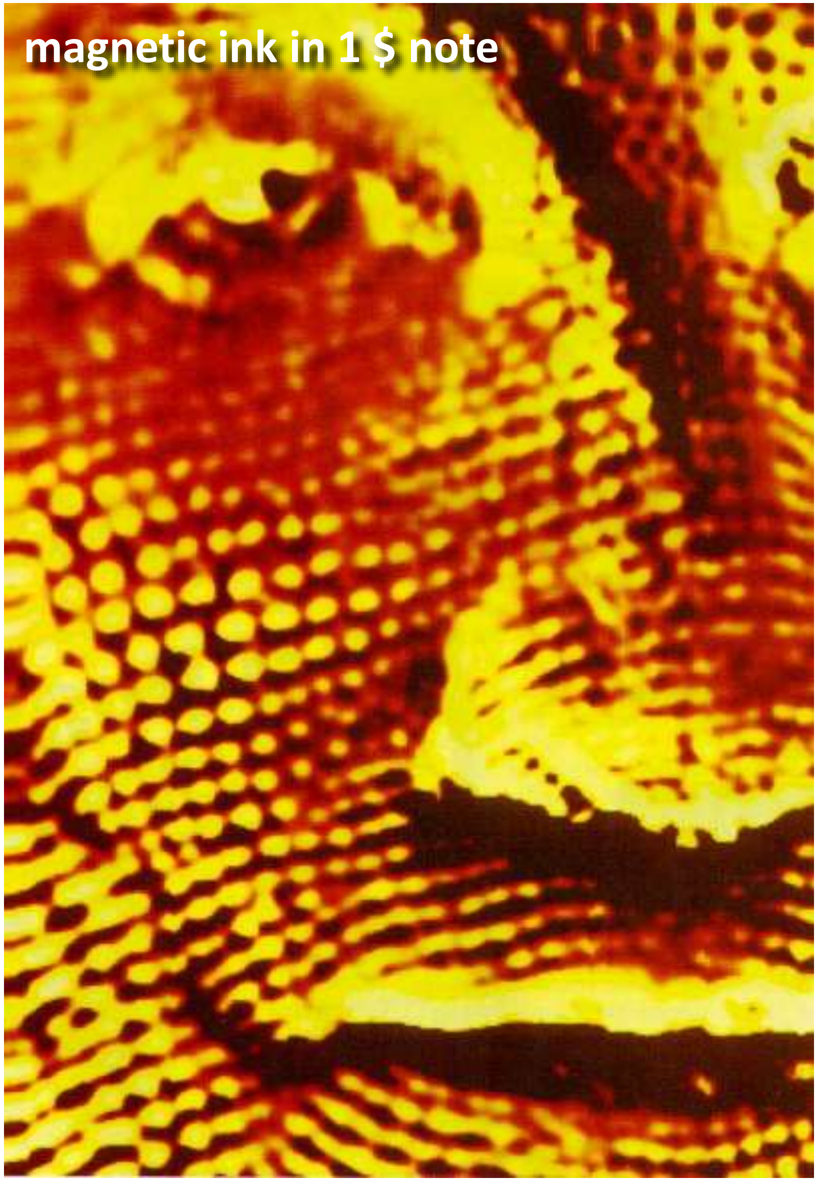

4.5.3 nano-SQUID Microscopy

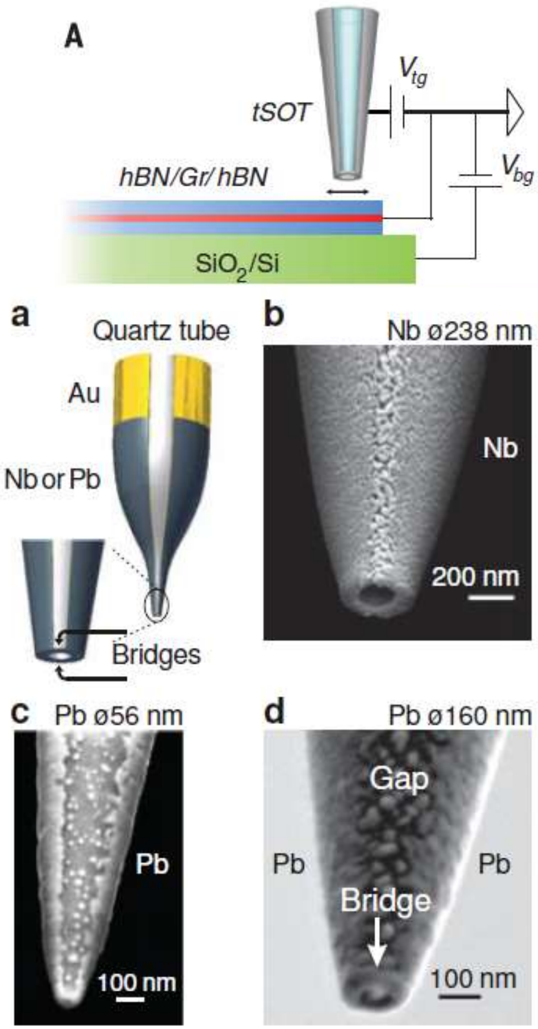

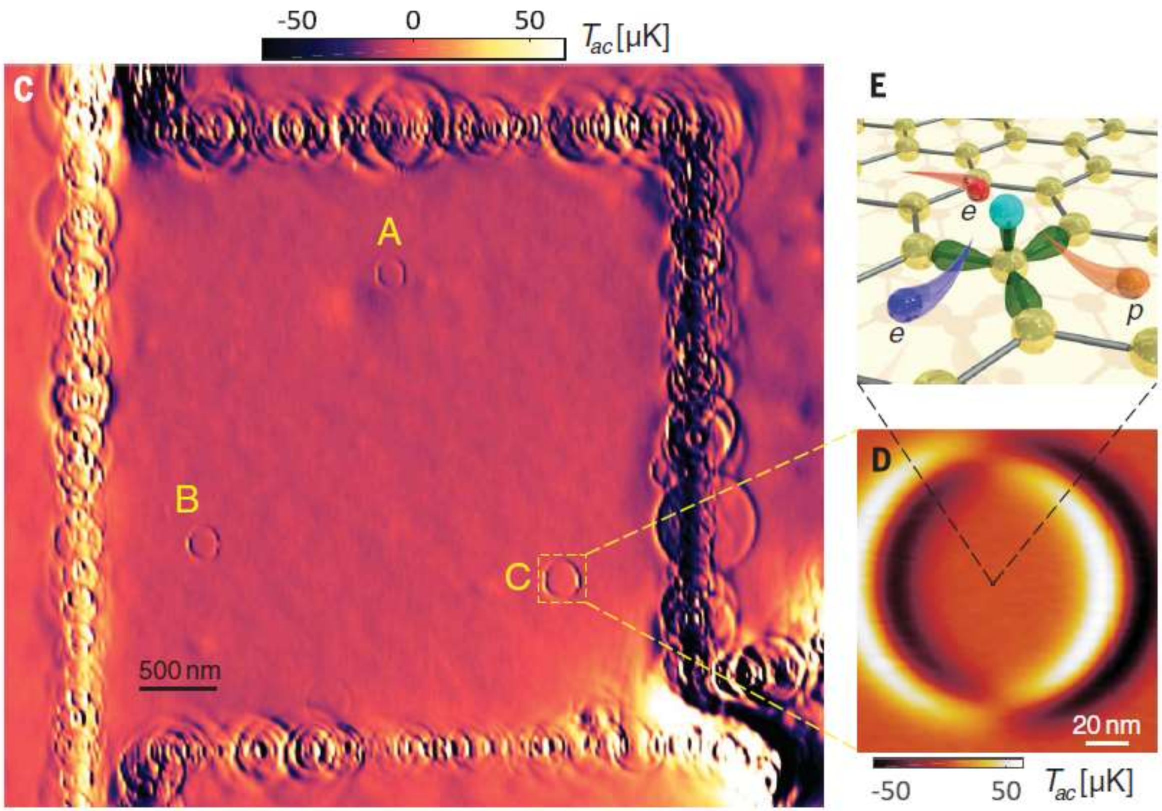

→ Scanning nano-SQUIDs
Illustration of an atomic defect in graphene that creates a localized resonant dissipative state at the center of the ring (D), which in turn mediates inelastic scattering of an impinging electron

D. Vasyukov et al., *Nature Nanotechnology* **8**, 639–644 (2013)
D. Halbertal et al., Science **358**, 1303-1306 (2017).

4.5.4 Gravity wave antennas and gravity gradiometers

Motivation:

Inertial navigation, general relativity, deviations from r^{-2}-law, and gravitational waves:

→ E.g., collapsing stars, rotating double stars

→ Expansion and contraction oscillations

→ Expected length change $\frac{\delta\ell}{\ell} \simeq 10^{-19}$

→ Required resolution $\simeq 10^{-21}$

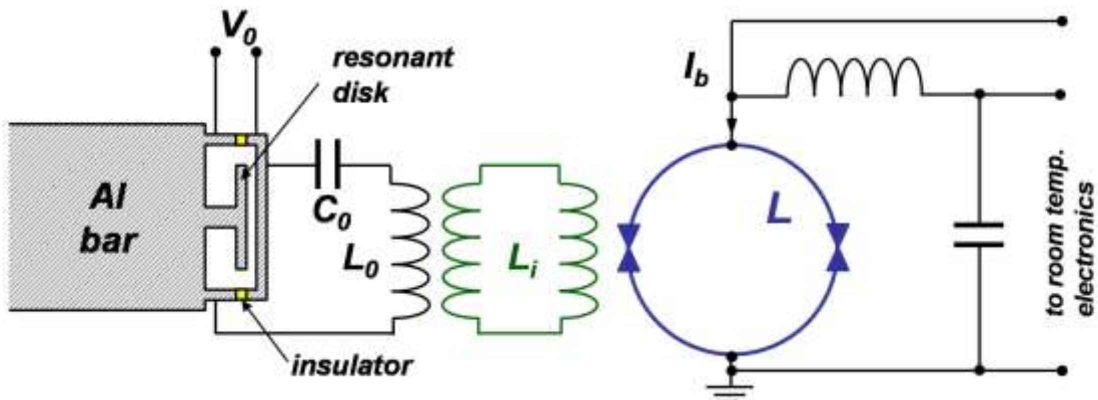

Resonant mass transducer from displacement to current

→ Antenna in the mK regime

→ Required resolution

→ Zero point motion

→ Quantum limited antenna!

→ Typical resonance frequency $\simeq 1\ \mathrm{kHz}$ → $T < \frac{\hbar\omega_\mathrm{ant}}{k_\mathrm{B}} \approx 50\ \mathrm{nK}$ → Impractical

→ Increase effective noise temperature T_eff by increasing Q

→ Gravitational pulse of length τ & antenna decay time $\frac{Q}{\omega_\mathrm{ant}}$ → $T_\mathrm{eff} = T\frac{\tau}{Q/\omega_\mathrm{ant}}$

→ Quantum limit (bar energy $\hbar\omega_\mathrm{ant} > k_\mathrm{B}T_\mathrm{eff}$) → Cool below $T < \frac{Q\hbar}{\mathrm{k}_B\tau}$

→ for $Q = 2\times 10^6$ and $\tau = 1\ \mathrm{ms}$ → $T \simeq 20\ \mathrm{mK}$

→ Quantum limited sensor is required

→ Present sensitivities $\frac{\delta\ell}{\ell} \simeq 10^{-18}$

→ 2015 → Gravitational wave reported in LIGO (laser interferometer, no SQUID)

Gravity gradiometer

Gravity gradient → Separation of test masses → Coil induction

→ Map earth's gravity gradient

→ Test of r^{-2} law

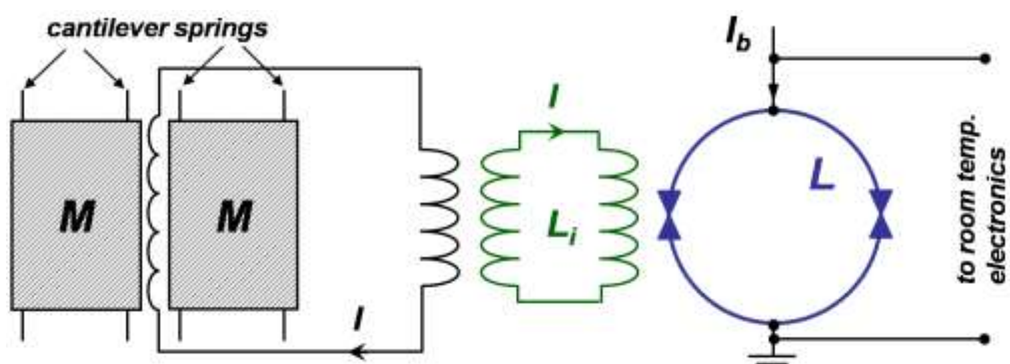

4.5.5 Geophysics

SQUIDs used to probe the magnetic properties of earth

- Rock magnetometry
- Mapping earth magnetic field / em impedance
- Geophysical surveying
- Archeology

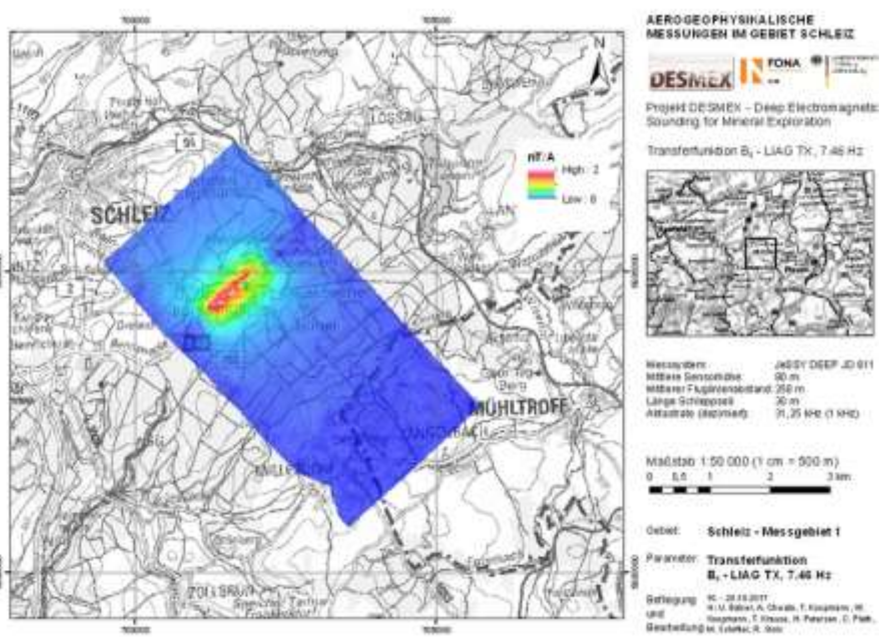

Supracon SQUID detector

4.5.5 Geophysics

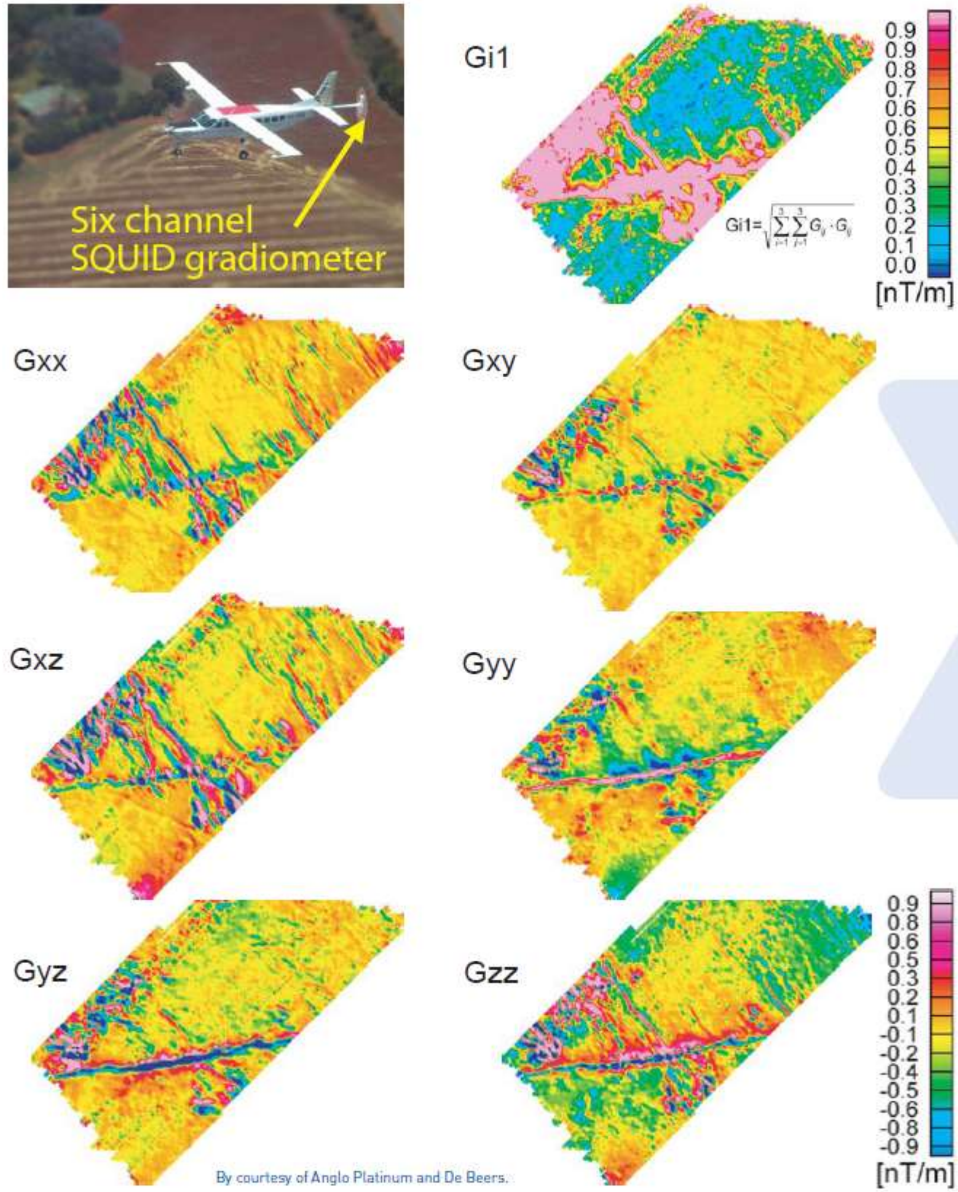

Supracon
SQUID detector

Summary (dc SQUID)

Negligible screening $\beta_L = 2LI_c/\Phi_0 \ll 1 \rightarrow \Phi \approx \Phi_{ext}$

$$I_s^m = 2I_c \left|\cos\left(\pi \frac{\Phi_{ext}}{\Phi_0}\right)\right|$$

Strong damping:

$$\langle V(t)\rangle = I_c R_N \sqrt{\left(\frac{I}{2I_c}\right)^2 - \left[\cos\left(\pi\frac{\Phi_{ext}}{\Phi_0}\right)\right]^2}$$

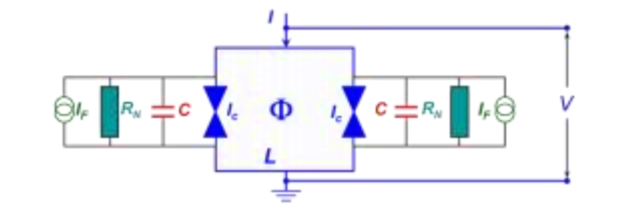

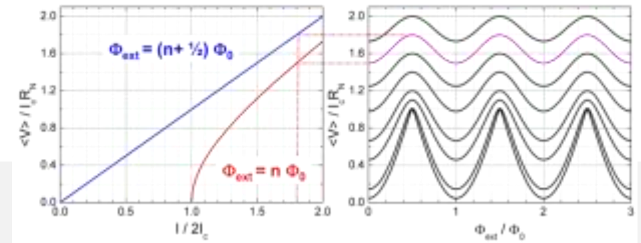

Large screening $\beta_L = 2LI_c/\Phi_0 \gg 1 \rightarrow \Phi = \Phi_{ext} + LI_{cir} \approx n\Phi_0$

$$I_s^m = 2I_c - \frac{2\Phi_{ext}}{L} = 2I_c\left(1 - \frac{2\Phi_{ext}}{\Phi_0}\frac{1}{\beta_L}\right)$$

Intermediate $\beta_L \rightarrow I_s^m(\Phi_{ext})$ self-consistently from $\Phi(\Phi_{ext})$ and $I_s^m(\Phi)$

Performance

$$H \equiv \left|\left(\frac{\partial V}{\partial \Phi_{ext}}\right)_{I=const}\right| \qquad S_\Phi(f) = \frac{S_V(f)}{H^2} \qquad \epsilon(f) = \frac{S_\Phi(f)}{2L} = \frac{S_V(f)}{2LH^2}$$

Optimum operation ($\beta_L \approx 1$, $\beta_C \approx 1$):

$$\epsilon(f) \simeq 16k_BT\sqrt{\frac{LC}{\beta_C}} \simeq \frac{16\sqrt{\pi}k_BT}{\omega_p}$$

Operation in flux-locked-loop as null detector

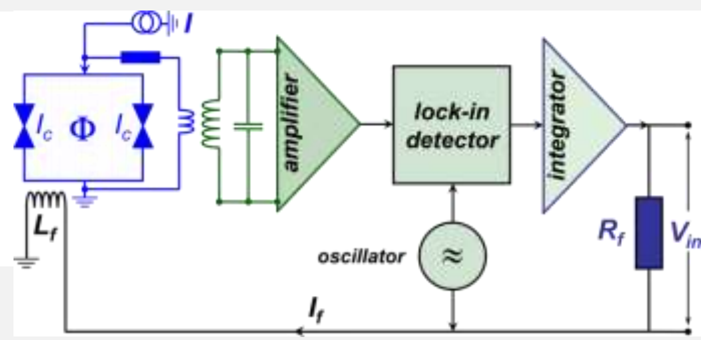

Summary (rf-SQUID)

$$\frac{\Phi}{\Phi_0} = \frac{\Phi_{\mathrm{ext}}}{\Phi_0} - \frac{\beta_{L,\mathrm{rf}}}{2\pi} \sin\left(2\pi\frac{\Phi}{\Phi_0}\right)$$

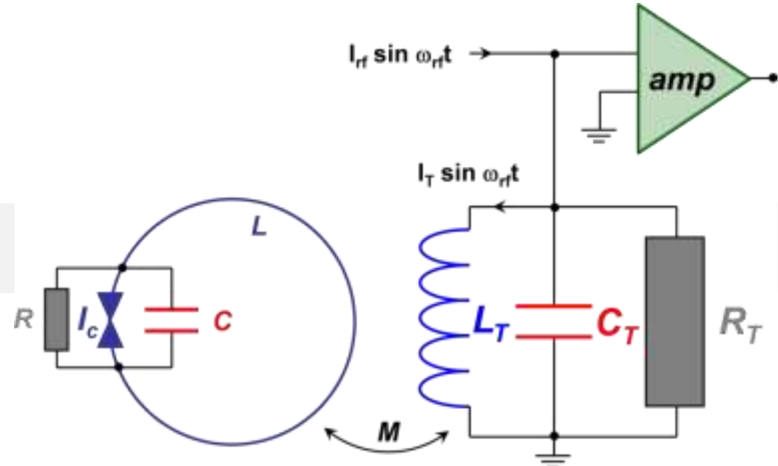

Operation → inductive coupling to tank circuit

Performance:

$$H \equiv \left| \left(\frac{\partial V_T}{\partial \Phi_{\mathrm{ext}}}\right)_{I_{\mathrm{rf}}=const} \right| \simeq \frac{\omega_{\mathrm{rf}} L_T}{M}$$

$$S_\Phi \approx \frac{(L I_c)^2}{\omega_{\mathrm{rf}}} \left(\frac{2\pi k_B T}{I_c \Phi_0}\right)^{4/3} \qquad \epsilon \approx \left(\frac{\pi \eta^2 \Phi_0^2}{2L} + 2\pi\eta k_B T_{\mathrm{amp}}^{\mathrm{eff}}\right)\frac{1}{\omega_{\mathrm{rf}}}$$

Operation in flux-locked-loop as null detector

Summary (SQUID based instruments)

Antenna, SQUID (flux-to-voltage transformer), read-out electronics
Magnetometer, gradiometer, voltmeter, susceptometer, …
Magnetic field resolution: few $fT/(Hz)^{1/2}$
Application: magnetocardiography/-encephalography, NDE, microscopy, geophysics